

AFWL TR-65-11

AFWL
TR
65-11

SIMULATION OF AIR-BLAST-INDUCED GROUND MOTION

Phase I

by

Gerald P. D'Arcy
Captain USAF

Harry E. Auld
Captain USAF

Gerald G. Leigh
Captain USAF

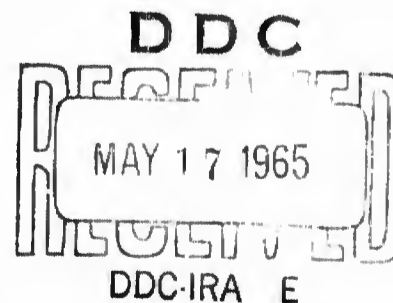


COPY	<u>2</u>	OF	<u>3</u>	<u>81e</u>
HARD COPY	\$. 3.00			
MICROFICHE	\$. 0.75			

Research and Technology Division
AIR FORCE WEAPONS LABORATORY
Air Force Systems Command
Kirtland Air Force Base
New Mexico

TECHNICAL REPORT NO. AFWL TR-65-11

April 1965



ARCHIVE COPY

AFWL TR-65-11

Research and Technology Division
AIR FORCE WEAPONS LABORATORY
Air Force Systems Command
Kirtland Air Force Base
New Mexico

When U. S. Government drawings, specifications, or other data are used for any purpose other than a definitely related Government procurement operation, the Government thereby incurs no responsibility nor any obligation whatsoever, and the fact that the Government may have formulated, furnished, or in any way supplied the said drawings, specifications, or other data, is not to be regarded by implication or otherwise, as in any manner licensing the holder or any other person or corporation, or conveying any rights or permission to manufacture, use, or sell any patented invention that may in any way be related thereto.

This report is made available for study with the understanding that proprietary interests in and relating thereto will not be impaired. In case of apparent conflict or any other questions between the Government's rights and those of others, notify the Judge Advocate, Air Force Systems Command, Andrews Air Force Base, Washington, D. C. 20331.

DDC release to OTS is authorized.

BLANK PAGE

AFWL TR-65-11

SIMULATION OF AIR-BLAST-INDUCED GROUND MOTION

Phase I

by

Gerald P. D'Arcy
Captain USAF

Harry E. Auld
Captain USAF

Gerald G. Leigh
Captain USAF

April 1965

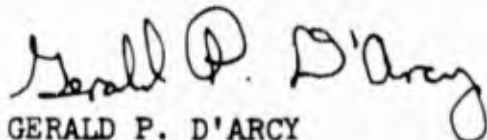
FOREWORD

The work reported here was performed under Project 5710, Program Element 7.60.06.01.5, from December 1963 to August 1964. The manuscript was submitted 24 March 1965 by the program monitor, Captain Gerald P. D'Arcy, WLDC.

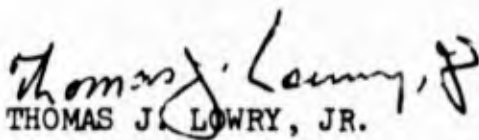
This research has been funded by the Defense Atomic Support Agency under WEB No. 13.166.

The authors of this report acknowledge the contributions made by Lieutenants R. A. Zang and Dwayne D. Piepenburg, who designed and procured much of the test hardware. These two officers also assisted in the design of the various experiments.

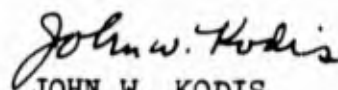
This technical report has been reviewed and is approved.



GERALD P. D'ARCY
Captain USAF
Project Officer



THOMAS J. LOWRY, JR.
Colonel USAF
Chief, Civil Engineering
Branch



JOHN W. KODIS
Colonel USAF
Chief, Development
Division

ABSTRACT

An analytical and experimental program was performed to determine the most promising techniques for simulating the air-blast-induced ground motions from a large-yield nuclear weapon. Two techniques were then selected for further development. One of the selected techniques employs a detonable gas mixture and the other a primacord matrix to generate a traveling shock wave which loads the ground. The nuclear air-blast overpressure environment is described and the simulation produced by either scheme is compared with this environment. The primacord technique was then selected because it was found to be the most practical and economical. Sufficient data are presented to enable the design of simulation experiments which use either technique.

This page intentionally left blank.

CONTENTS

<u>Section</u>		<u>Page</u>
I	INTRODUCTION	1
II	NUCLEAR AIR-BLAST ENVIRONMENT	3
III	AIR-INDUCED GROUND MOTIONS	5
IV	DETONABLE GAS SIMULATION TECHNIQUE	12
V	PRIMACORD SIMULATION TECHNIQUE	32
VI	CONCLUSIONS	50
	APPENDIX I	
	DURATION CALCULATIONS	51
	APPENDIX II	
	INSTRUMENTATION	58
	REFERENCES	69
	DISTRIBUTION	70

ILLUSTRATIONS

<u>Figure</u>		<u>Page</u>
1	Shock Parameters for a 1-Megaton Surface Burst	4
2	Side Effects Caused by Truncating the Area Loaded	7
3	Stress Waves in Elastic Half-Space	8
4	Air-Blast-Induced Ground Motion	10
5	Detonation Shock Discontinuity and Reaction Zone	13
6	Rankine-Hugoniot Curve for a 3 to 1 Molar Ratio Mixture of Hydrogen-Oxygen Initially at 12 psi and 298°K	14
7	Detonation Pressure versus Velocity for a 3 to 1 Molar Mixture of Hydrogen-Oxygen Initially at 12 psi and 298°K	16
8	Detonation Wave Expansion	17
9	Typical Detonation Wave Pressure--Time History	17
10	Initial Mixture Conditions Required to Simulate Air Shock Waves	19
11	Duration to Half Peak Pressure--Peak Pressure = 300 psig, Cavity Depth = 36 inches	20
12	Duration to Half Peak Pressure--Peak Pressure = 300 psig, Cavity Depth = 48 inches	21
13	Duration to Half Peak Pressure--Peak Pressure = 300 psig, Cavity Depth = 60 inches	22
14	Detonable Gas Facility	24
15	Detonable Gas Facility (Photograph)	25
16	Detonation Wave Photography	27
17	Duration to Half Pressure--Test No. 1	28
18	Test No. 1 Pressure Record	30
19	Two-Atmosphere Container	31
20	Primacord Simulation Technique	33
21	Peak Overpressure versus Loading Density	34
22	Shock Velocity versus Primacord Weave Angle	35
23	Duration to Half Peak Pressure--Peak Pressure = 300 psig	36
24	Duration to Half Peak Pressure--Peak Pressure = 400 psig	37

ILLUSTRATIONS (cont'd)

<u>Figure</u>		<u>Page</u>
25	Duration to Half Peak Pressure--Peak Pressure = 500 psig	38
26	Duration to Half Peak Pressure--Peak Pressure = 750 psig	39
27	Duration to Half Peak Pressure--Peak Pressure = 1,000 psig	40
28	Primacord Experiment No. 1	42
29	Primacord Experiment No. 3	43
30	Shock-Tube Piston Analogy	44
31	Typical Pressure Trace	46
32	Effect of Cavity Depth	49
33	Elemental Volume of Overburden	52

TABLES

<u>Table</u>		<u>Page</u>
I	Summary of One-Dimensional Wave Propagation Quantities	5
II	Results from Detonation Tests	29
III	Results from Primacord Tests	45
IV	Effect of Cavity Depth on Duration	47
V	Program Constants	54
VI	Phase I Instrumentation Equipment List	62

SYMBOLS

a	Atmospheric pressure
C	Velocity of stress wave in earth medium
C'	Velocity of side rarefaction
D_p^+	Positive phase duration of a pressure pulse
E_o	Internal energy of reactants
E_l	Internal energy of products
g	Acceleration due to gravity
h	Time increment of integration
I	Impulse
M	Weight of overburden, one-dimensional modulus
m_o, m_1, m_2, m_3	Coefficients used in numerical integration
P	Cavity pressure
P_o	Initial pressure of reactants
P_l	Detonation pressure
$P(t)$	Input pressure at surface of earth
$P(t - z/c)$	Input pressure with time transformation
psia	lb/in ² absolute
psig	lb/in ² gauge
Q	Heat liberated from chemical reaction
T_o	Temperature of reactants
T_l	Detonation temperature
U	Shock velocity, detonation velocity
u	Detonation wave particle velocity
u_z	Earth displacement in z direction
\dot{u}_z	Earth particle velocity in z direction

SYMBOLS (cont'd)

\ddot{u}_z	Earth acceleration in z direction
V	Cavity volume at some time t
V_0	Initial cavity volume
X	Molar ratio of mixture, $\frac{\text{moles hydrogen}}{\text{moles oxygen}}$ overburden displacement.
\dot{X}	Acceleration of overburden
X_0	Initial cavity displacement
Z	Vertical location of particle
α	Angle at which the stress wave enters the earth
β	Primacord weave angle
γ	Ratio of specific heats
ϵ_z	Strain in z direction
ρ	Mass density of earth medium
ρ_0	Density of the reactants
ρ_1	Density of the products
σ_z	Normal stress in z direction

SECTION I

INTRODUCTION

The Air Force has a requirement to evaluate the survivability and the vulnerability of its hardened, operational structures. The requirement for this evaluation is twofold. First, this information is necessary to provide a realistic basis for evaluation and planning of hardened facilities; second, such a program may reveal design or construction deficiencies that can be corrected to increase a facility's hardness. The moratorium imposed by the Test Ban Treaty of August 1963 has ruled out the possibility of testing operational facilities in an actual nuclear environment. Therefore, the Air Force Weapons Laboratory initiated a project to develop methods to simulate the air-blast-induced ground motions caused by large-yield nuclear weapons. This project is to be accomplished in three phases. The objective of the first phase, which is described in this report, was to develop a suitable simulation technique. Phase II consisted of a large-scale field experiment to demonstrate the feasibility of scaling up the relatively small Phase I experiments and to define the mass of earth realistically affected by the shock pulse. Phase III will be a proof test of an operational hardened facility.

At the onset of this project, several simulation techniques or schemes were considered. However, most of these techniques were quickly eliminated by considering the accuracy of the simulation produced by each. Some of the techniques rejected as a result of this study were FAX, high explosives placed in an array, hemispherical source of high explosives, and a buried shock tube. After this elimination process was completed, two techniques appeared worthy of further development. This technical report is a description of the parallel programs initiated to develop these two techniques.

The two most promising methods are the detonable gas technique and the primacord technique. The idea behind the detonable gas technique is to select a combustible mixture of gases that will produce a detonation wave with the same pressure and velocity as a similar shock wave in air. The gas mixture is then confined in a flexible container which is placed over the surface of the ground. An overburden is placed over the container to

obtain a greater duration of the pressure pulse. Finally, the container is ignited along one edge, and a detonation wave moves through the container and over the surface of the ground. In the primacord technique, a wooden structure buried beneath an overburden forms a cavity in which is suspended a matrix of primacord. The primacord has a burning rate greater than 20,000 feet per second. By varying the placement angle in the matrix, different frontal velocities can be simulated. The combustion products from the burning primacord are released along the length of the cavity at a rate which is proportional to the placement angle. These products act as a piston which drives a shock out ahead into the air. The intense, short-duration shocks generated by the detonating primacord overtake the main shock and reinforce it. This produces a natural decay during the early part of the pressure pulse. If the cavity size were fixed, the pressure in the cavity would soon settle down to the equilibrium pressure of the combustion products. However, the overburden begins to move, due to the force of the expanding gases. This expansion causes a gradual pressure reduction which simulates the later blast-wave decay.

This report will first discuss the actual nuclear environment and the associated ground motion. Next, the detonation technique will be described along with experimental results. Then the primacord technique will be described. Finally, the two techniques will be compared. Two appendixes are included. Appendix I is a description of the method used to predict the duration of the simulated air-blast overpressure pulse. Appendix II is a description of the instrumentation used during the Phase I experiments. This report also presents information which will allow the design of simulation experiments which use either techniques.

SECTION II

NUCLEAR AIR-BLAST ENVIRONMENT

Figure 1 illustrates the pressure decay with radial distance from a 1-megaton surface explosion. The rate of pressure decay decreases with radius. At 1,500 feet from a 1-megaton weapon the overpressure is 1,000 psig. At 1,850 feet the pressure has dropped to 500 psig and at 2,200 feet the pressure has decreased to 300 psig. In this total distance of 700 feet between the 1,000- and 300-psig pressure levels, the corresponding shock front velocity has decreased from 8,600 feet per second to 4,800 feet per second. The total impulse contained in the air blast at 1,500 feet is 55 lb-sec/in² as compared with 32 lb-sec/in² at 2,200 feet.

A number of blast wave parameters should be noted. These parameters are as follows:

1. Peak overpressure
2. Shock velocity
3. Wave shape
4. Shock pressure decay with radius

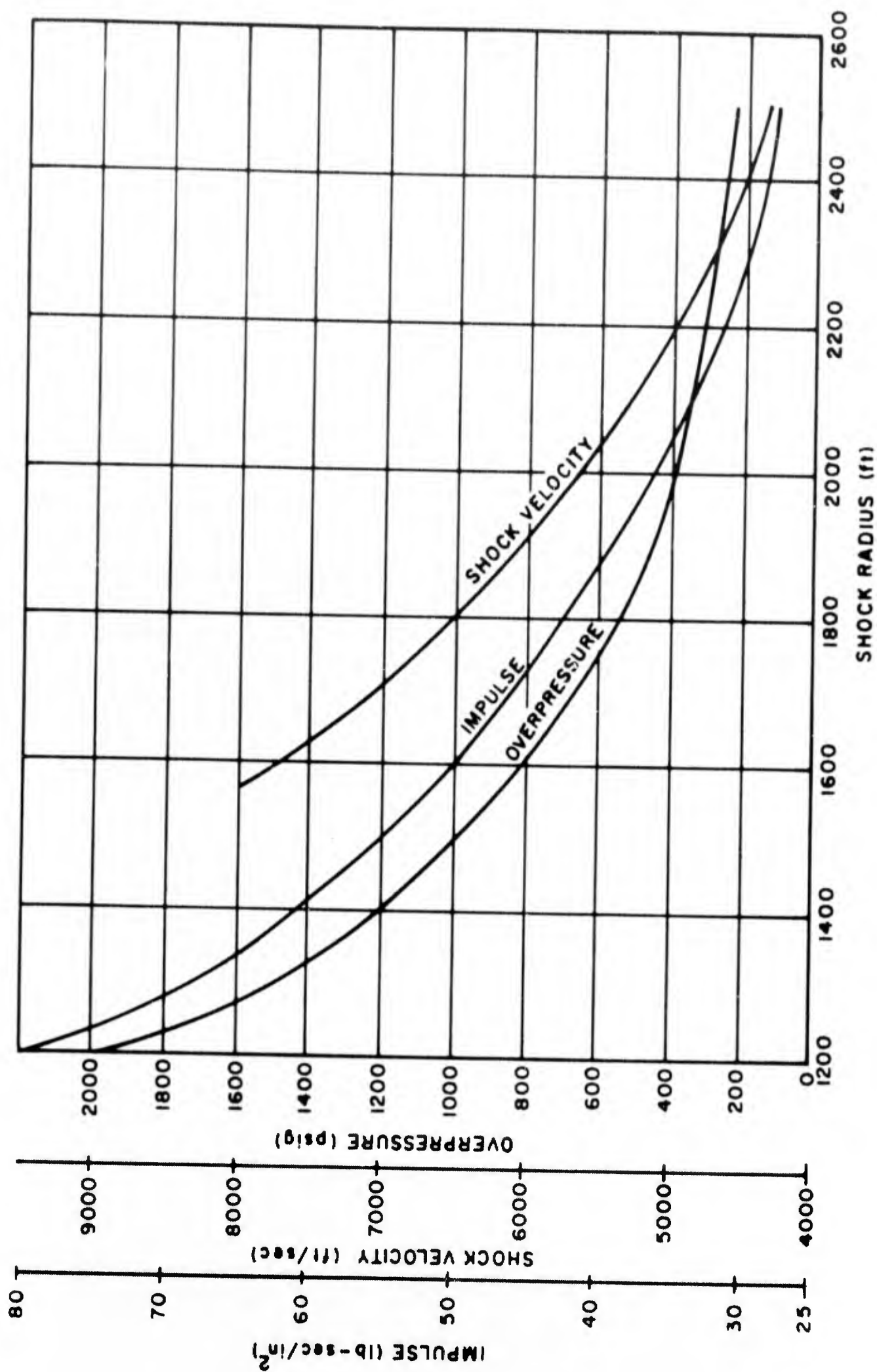


Figure 1. Shock Parameters for a 1-Megaton Surface Burst

SECTION III

AIR-INDUCED GROUND MOTIONS

Simple one-dimensional elastic wave theory can be used to establish relationships between stress, displacement, strain, velocity, and acceleration in the earth resulting from an air-blast wave. Although this theory is highly idealized, it can provide an understanding of the basic relationships between the air-blast parameters and the stresses and motions induced in the soil. These results can then be corrected to take account of the other factors which influence the free-field behavior. Table I summarizes the one-dimensional wave propagation quantities.

Table I

SUMMARY OF ONE-DIMENSIONAL WAVE PROPAGATION QUANTITIES

<u>Quantity</u>	<u>Equation</u>
Stress	$\sigma_z = -P(t - z/C)$
Strain	$\epsilon_z = -P(t - z/C)/\rho C^2$
Particle velocity	$\dot{u}_z = P(t - z/C)/\rho C$
Particle acceleration	$\ddot{u}_z = \frac{1}{\rho C} \frac{\partial}{\partial t} [P(t - z/C)]$
Particle displacement	$u_z = I/\rho C$

where

σ_z = normal stress in z direction, tension considered positive

z = undisturbed location of a given particle, downward considered positive

$-P(t)$ = input pressure at the surface, $z = 0$

C = velocity of the stress wave in the medium

$-P(t - z/C)$ = input pressure with time transformation (z/C is the time it takes the wave to propagate to the depth of interest)

ϵ_z = strain in z direction, tensile strain considered positive

ρ = mass density of the medium

\dot{u}_z = particle velocity in z direction

\ddot{u}_z = particle acceleration in z direction

u_z = particle displacement in z direction

I = integral of pressure-time curve at time of interest

One-dimensional elastic theory shows that the stress in the soil propagates with an unaltered wave shape from the air-blast input. In reality three major changes take place as the stress wave propagates with depth. The rise time will increase, the impulse duration will be spread out, and the peak stress will decrease. Nonlinearities in the stress-strain curves of earthen materials are the primary cause of the first two factors. The variation in stress intensity with depth is caused by three separate phenomena. First, most earthen materials have highly nonlinear stress-strain curves which result in energy absorption. Second, when finite areas are loaded by transient inputs, rarefaction waves propagate inward from the boundaries (see figure 2). Third, spatial attenuation, or the spreading out of the load, results in reduced stresses at increasing depths. The first two phenomena must be studied experimentally; however, the third can be examined by considering an elastic half-space loaded by a realistic air-blast input (see figure 3). As previously described, the overpressure and shock velocity of the air-blast input are both decaying with radius. Each pressure level has a ray path along which it propagates and spatial divergence causes it to attenuate as it propagates. If a vertical section is examined, it can be shown that energy from higher overpressure regions will propagate into a radius of interest and locally reinforce the stress level. For a realistic air-blast input, the loading function parameters are changing at the appropriate rate to balance the effect of the spatial divergence at shallow depths, and no attenuation due to this effect takes place. Thus, the stress, which propagates to any depth z, is a function of the air-blast input, the size of the area loaded, and the properties of the medium.

The one-dimensional wave theory also shows that the strain and the particle velocity are affected by the magnitude and the wave shape of the air-blast input and the properties of the medium. These quantities are

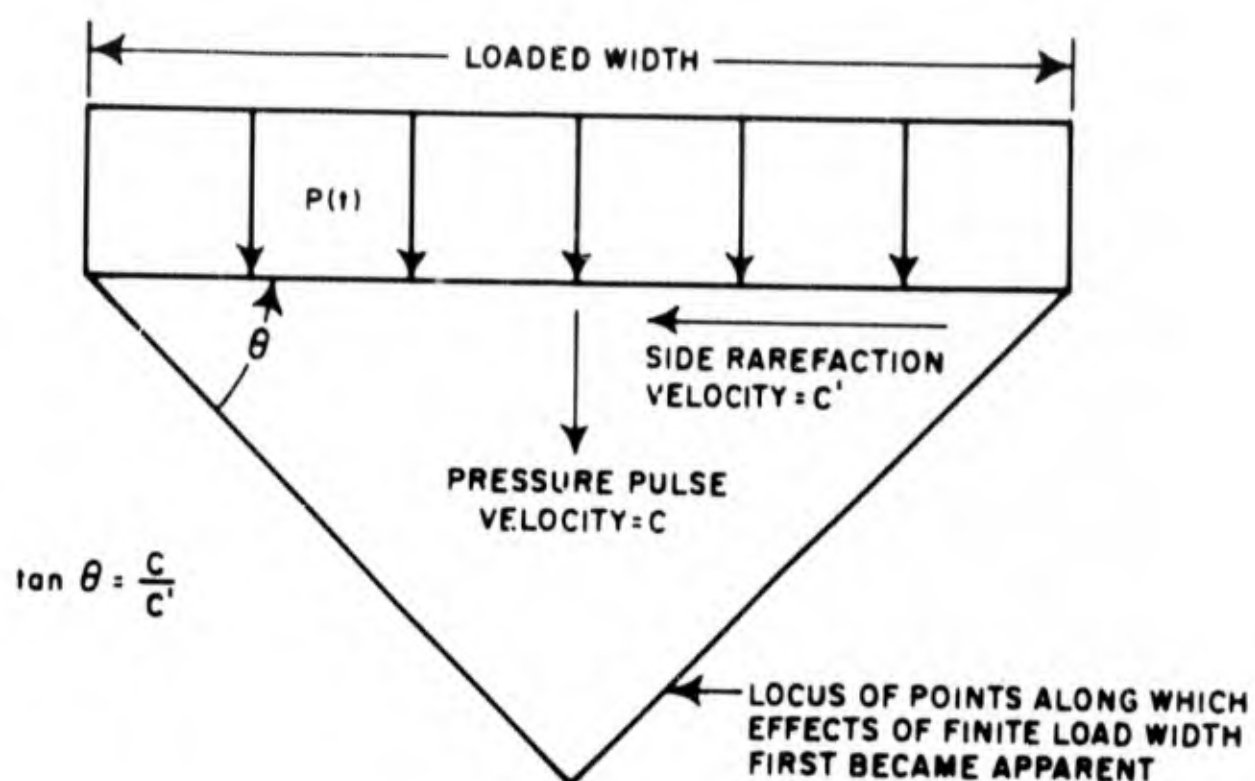


Figure 2. Side Effects Caused by Truncating the Area Loaded

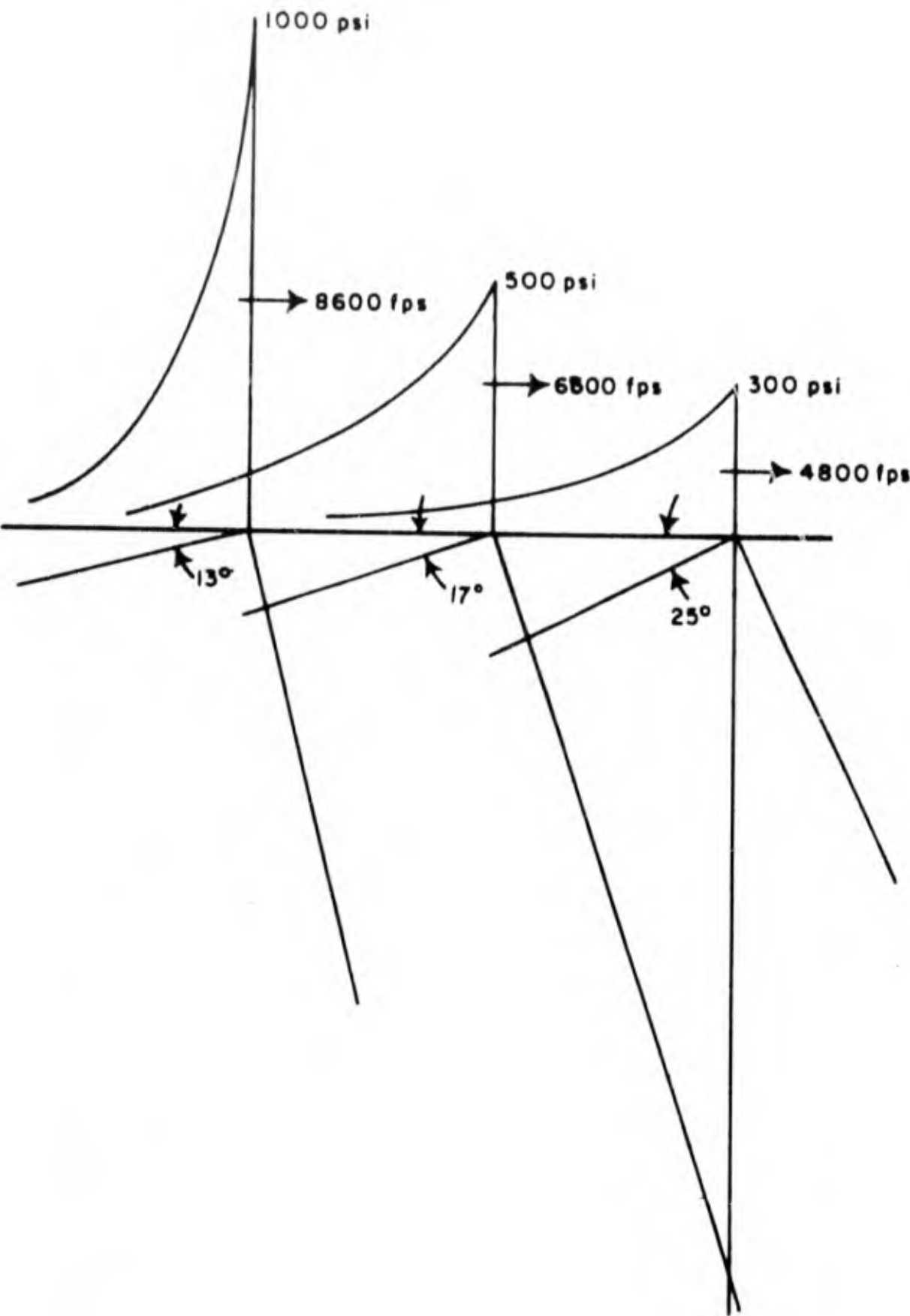


Figure 3. Stress Waves in Elastic Half-Space

affected by the same parameters which cause the attenuation of stress with depth. Acceleration is extremely sensitive to the initial shape of the air-blast input, particularly the rise time which increases with depth. Displacement depends on the impulse, which is defined by the integral of the stress-time history at the depth of interest. To realistically simulate displacements from a nuclear detonation, the impulse must match that of the nuclear explosion and the area loaded must be significantly large, in relationship to the depth of interest, to minimize the effect of rarefaction waves.

Only vertical components have been discussed thus far. A traveling wave must be considered to study the relationship between vertical and horizontal stresses and motion. Figure 4 illustrates a typical air-blast input, $P(t)$, traveling on the surface of the earth with a shock front velocity, U . The velocity of the stress wave into the earth, C , is determined by the intensity of the air-blast input and the properties of the earth materials. It is given by

$$C = \frac{M}{\rho C^2} \quad (1)$$

where

M = modulus obtained from a one-dimensional test at stress level of interest

ρ = mass density

In this report only the superseismic region, where the air shock velocity, U , is greater than the earth stress velocity, C , will be considered. This assumption is not overly restrictive since most hardened facilities are constructed in soil or soft rock to withstand high overpressures. At these high pressure levels, the stress wave trails behind the air-blast shock front and enters the ground with an angle α , which is defined by the equation

$$\sin \alpha = \frac{C}{U} \quad (2)$$

As indicated in figure 4, the initial earth motion is perpendicular to the stress wave front. Behind the front, the primary motion has a direction which lies between this initial angle and a vertical line. The components of either stress or motion can be approximated in a highly superseismic

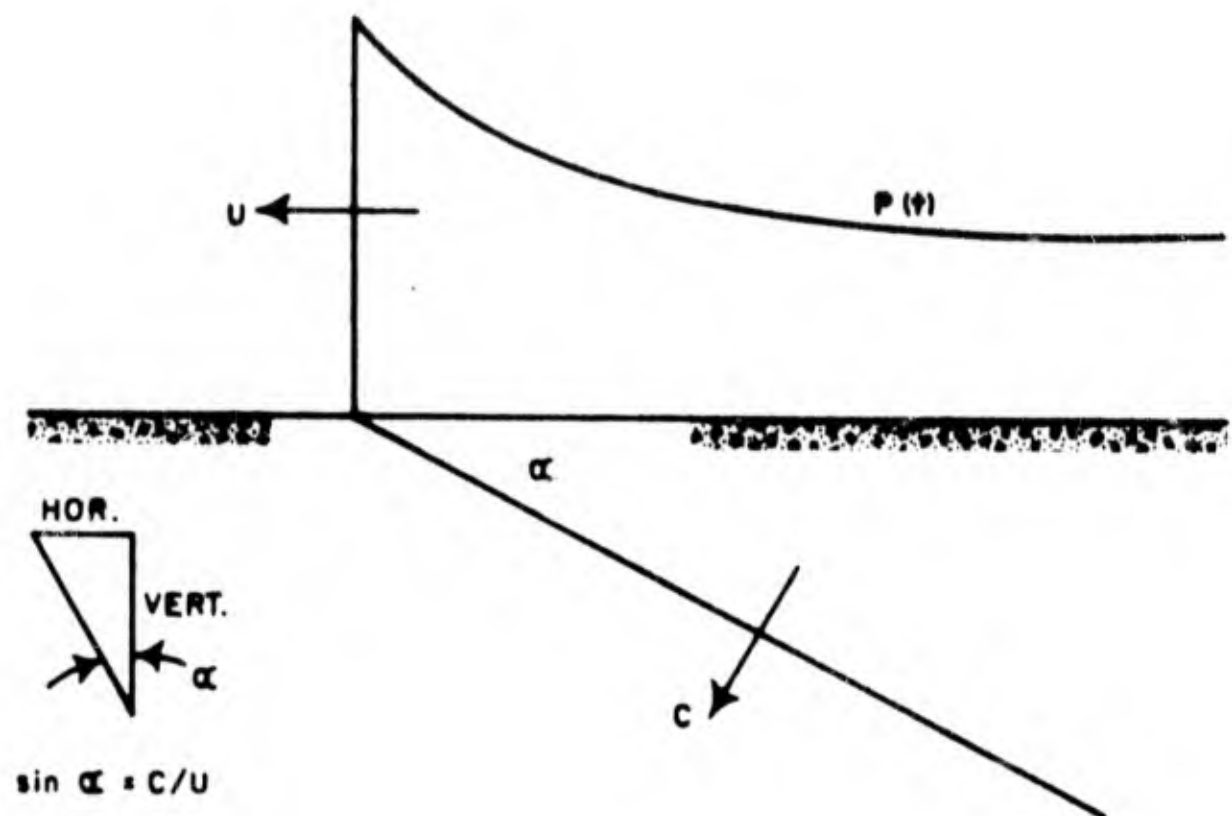


Figure 4. Air-Blast-Induced Ground Motion

region by

Horizontal component = value perpendicular to front $\times \sin \alpha$

Vertical component = value perpendicular to front $\times \cos \alpha$

Thus, the ratio of horizontal to the vertical component of stress and motion is a function of both the air-blast input and the material properties. This ratio is significant in determining free-field behavior and the loading on buried structures.

The purpose of this discussion of air-blast-induced ground motion is to show that the peak overpressure, shock-front velocity, and wave shape are significant parameters in defining the environment to be simulated. In addition, the size of the loaded area greatly influences the attenuation of motion and stresses with depth.

Provided a sufficiently large area is loaded, the peak stresses and particle velocities in the soil can be reasonably duplicated since the correct peak overpressure is applied to the surface of the soil. The peak accelerations in the soil will also be approximated fairly well since the rise time and the initial decay immediately behind the peak of the detonation wave and the air-blast input are nearly identical. The ratio of horizontal to vertical motions and stresses will be simulated since the appropriate shock-front velocity is produced. However, the displacements in the soil will be smaller than those found in an actual nuclear blast since a truncated area is being loaded and the entire impulse of the actual case cannot be duplicated.

SECTION IV

DETONABLE-GAS SIMULATION TECHNIQUE

The idea of simulating an air shock with a detonation was first investigated by the Stanford Research Institute (reference 1). A traveling detonation wave in a small facility was produced utilizing a detonable gas mixture. However, mixtures were used that yielded detonation velocities too high for realistic simulation, because near stoichiometric mixtures of gases were used.

Likewise, investigators at the Air Force Shock Tube Facility, Kirtland Air Force Base, New Mexico, did a small amount of research on the concept. They did not attempt to obtain a traveling wave since they were only interested in obtaining a technique for loading large soil areas to high pressures.

The Air Force Weapons Laboratory became interested in this simulation technique after an investigation showed that the correct detonation velocity could be obtained for a wide range of overpressures. This was done by computing detonation properties for a wide range of initial gas mixtures and pressures. These calculations are reported in reference 2.

As stated earlier, the concept behind this technique is the substitution of a detonation wave for an air-blast wave. One may regard the detonation wave as being headed by a shock front, which advances with a constant velocity into the unconsumed explosive, and is followed by a zone of chemical (reference 3). This assumption agrees very well with observation and allows hydrodynamic methods to be applied to the problem. That is, the detonation shock is treated as a discontinuity and the conservation of energy and momentum along with the continuity equations are assumed to be valid across this discontinuity. Figure 5 schematically shows a detonation wave propagating into a combustible mixture. The subscript zero refers to the initial conditions of the reactants. It is assumed that the properties of the mixture change instantly to P_1 , T_1 , ρ_1 , E_1 behind the shock. Then, by assuming a coordinate system that moves with the shock front, the hydrodynamic equations may be written:

$$\rho_0 U = \rho_1 (U-u) \text{ (continuity)} \quad (3)$$

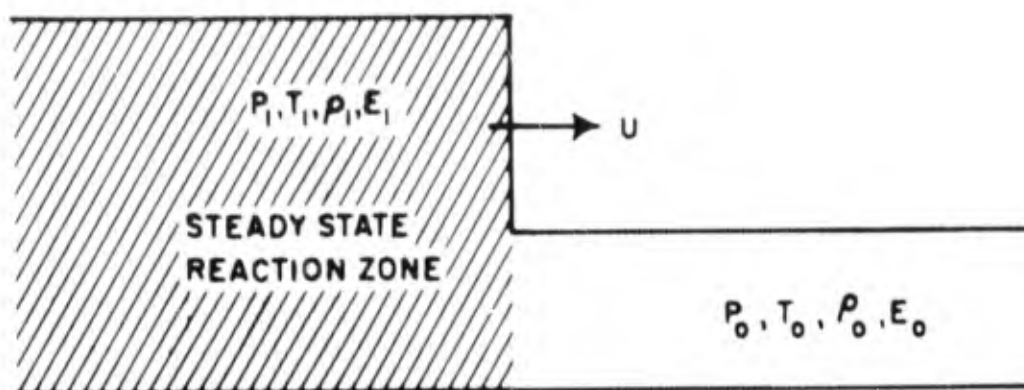


Figure 5. Detonation Shock Discontinuity and Reaction Zone

$$P_0 + \rho_0 U^2 = P_1 + \rho_1 (U-u)^2 \quad (\text{momentum}) \quad (4)$$

$$E_0 + \frac{P_0}{\rho_0} + \frac{1}{2} U^2 = E_1 + \frac{P_1}{\rho_1} + \frac{1}{2} (U-u)^2 \quad (\text{energy}) \quad (5)$$

where u is the particle velocity behind the front (reference 3).

These equations can be combined to give

$$\int_{T_0}^{T_1} C_v dT - Q = \frac{1}{2} (v_1 - v_0) (P_1 + P_0) \quad (6)$$

$$U = \rho_0 \sqrt{\frac{P_0 - P_1}{v_1 - v_0}} \quad (7)$$

$$(U-u) = \rho_1 \sqrt{\frac{P_0 - P_1}{v_1 - v_0}} \quad (8)$$

The specific heat in the integral refers to the products; the Q represents the heat liberated from the chemical reaction at temperature T_0 . The specific volume is denoted by v . Figure 6 is known as a Hugoniot curve and is a plot of equation 6. This particular Hugoniot is for a 3 to 1 molar ratio mixture of oxygen to hydrogen initially at a pressure of 12 psia. The missing portion of the Hugoniot curve is due to equations 7

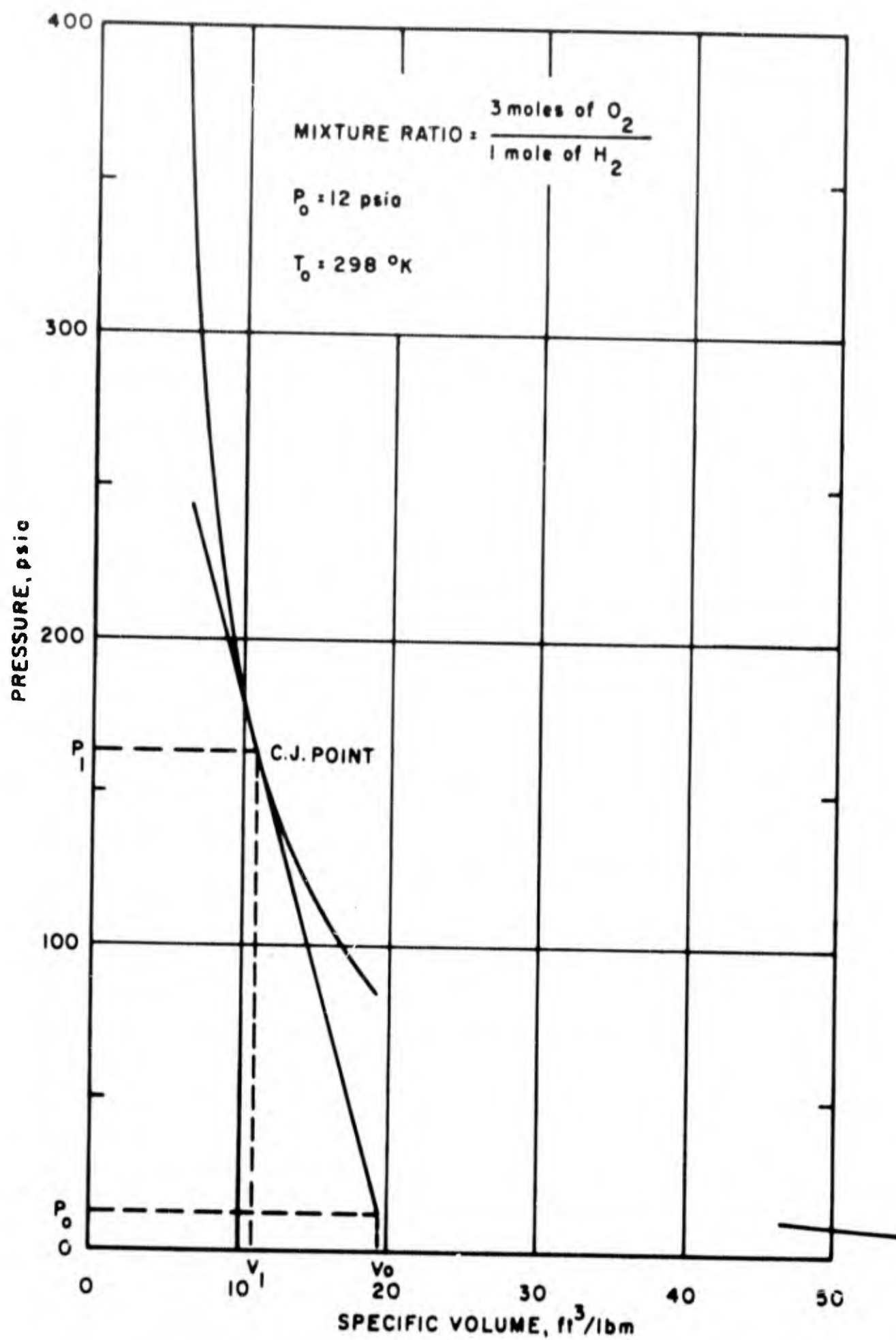


Figure 6. Rankine-Hugoniot Curve for a 3 to 1 Molar Ratio Mixture of Hydrogen-Oxygen Initially at 12 psi and 298°K

and 8 which indicate imaginary velocities for these values of P and v . The lower portion of the curve represents possible deflagration (combustion) and will not be considered in this report. The upper portion of the curve represents possible detonation pressures (reference 3).

The tangent point for a line shown from P_0, v_0 to the curve identifies the Chapman-Jouguet detonation pressure. Courant and Friedrichs (reference 4) offer a proof that this is the only stable detonation. The Hugoniot curve is tangent to the adiabatic curve at this point, and by equating the slope of the adiabat to the slope of the Hugoniot, it can easily be shown that the particle velocity relative to the front is equal to the local sound speed. Finally, it can be shown that the Chapman-Jouguet detonation is slowest of all detonation waves. Figure 7 is a plot of the velocity versus pressure expected from the above mixture.

Probably the most important fact to be derived from this discussion is that for a given mixture, a unique stable detonation pressure and velocity exists for each set of initial conditions. This means that the properties of the detonation front will be constant with time. On the other hand, the properties of gas behind the front will change with the distance that the detonation wave has traveled. This can easily be shown if we assume that a centered simple wave is following the detonation wave and that the expansion behind the front is isentropic. This derivation is shown in reference 2 and will lead to the result that

$$\frac{dx}{dt} = 68.1 \frac{P_1}{\gamma \rho_1} \left(\frac{2\gamma}{\gamma-1} \right) \left[\left(\frac{P}{P_1} \right)^{\frac{\gamma-1}{2\gamma}} - 1 \right] + U \quad (9)$$

where P_1 is in lb/in^2 , ρ_1 is in lbm/ft^3 , and U is in ft/sec . Figure 8 shows a graph of a centered, simple expansion. Observation has shown that a centered, simple wave approximates the expansion behind a detonating wave. Figure 9 is a pressure-time plot at a distance X from ignition. This figure is computed by selecting the desired distance from ignition of figure 8 and constructing a vertical line. The values of pressure versus time are then read off along this line. The straight lines in figure 8 result from

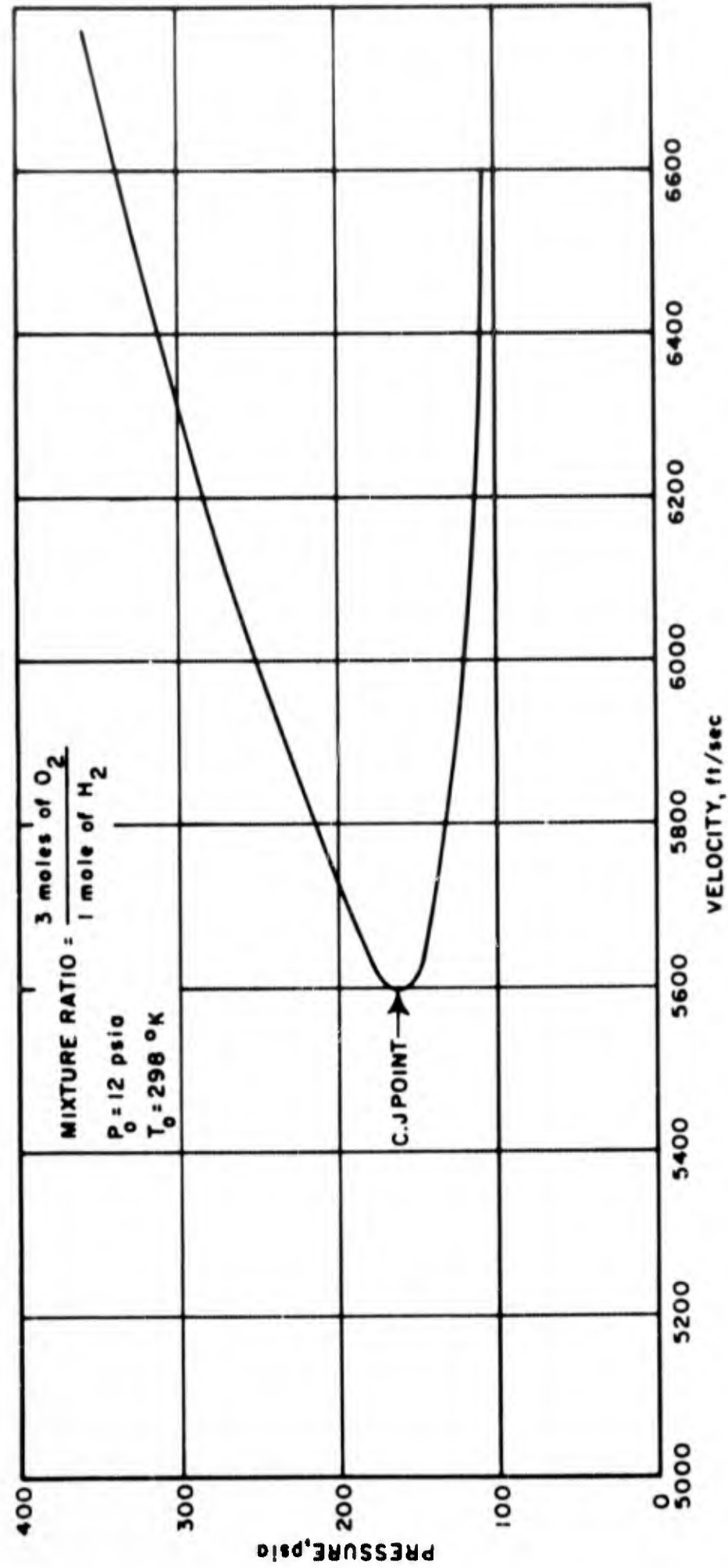


Figure 7. Detonation Pressure versus Velocity for a 3 to 1 Molar Mixture of Hydrogen-Oxygen Initially at 12 psi and 298°K

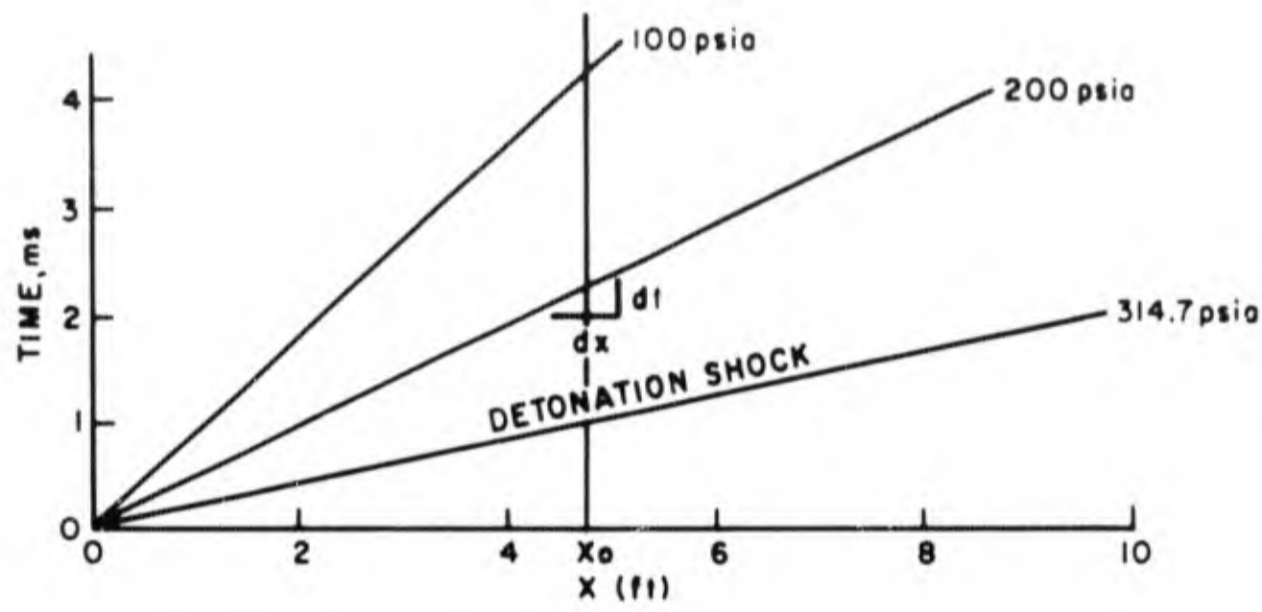


Figure 8. Detonation Wave Expansion

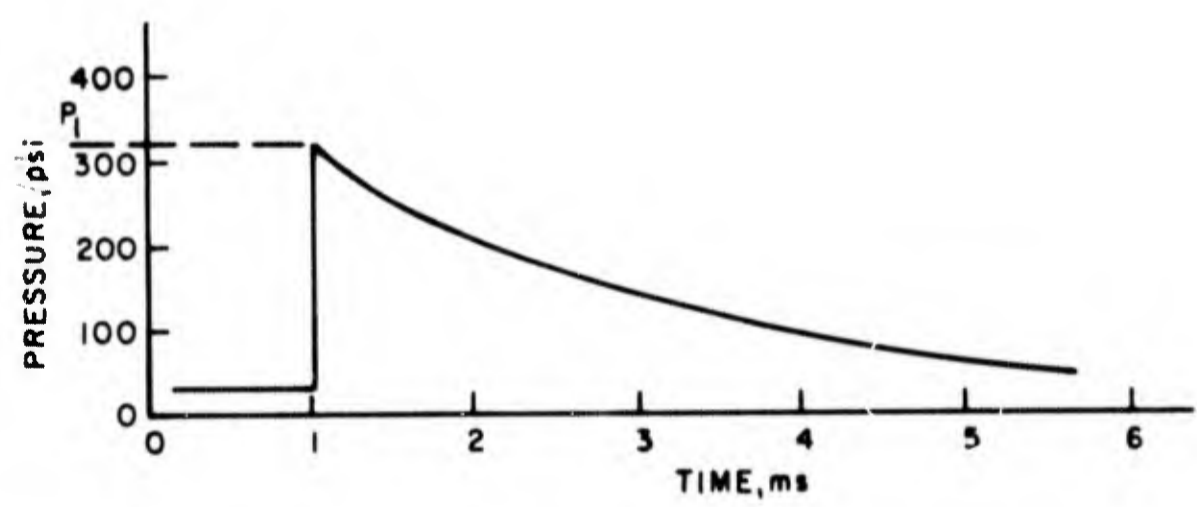


Figure 9. Typical Detonation Wave Pressure--Time History

the assumption of a simple, centered expansion and indicate that for this idealized expansion the growth of the pressure duration behind the shock is linear with distance, i.e., $D_p^+ = KX$. Therefore, a detonation wave propagates through a combustible mixture with a constant peak pressure and with a duration that grows linearly with distance.

Figure 10 shows the simulation possible with pure hydrogen-oxygen mixtures. These curves present the mixture ratios and the initial pressure required to simulate overpressures that vary between 300 psi to greater than 1,200 psi. These curves were determined experimentally in the 80-foot-long, 13-inch-diameter, high-pressure shock tube located at the Air Force Shock Tube Facility. The growth in pressure duration was observed along with the peak pressure and velocity. The experimental and theoretical work that was required to derive figure 10 are reported in reference 2.

Theoretically, it is possible to simulate the pressures from 300 psi to greater than 1,200 psi from any given yield weapon with hydrogen-oxygen mixtures by selecting a mixture from figure 10. This will give the desired pressure and shock velocity. Next, a detonation expansion can be calculated using equation 9. The results of these calculations are shown in figures 8 and 9. For a good approximation, γ may be assumed to be equal to 1.25. This calculation will determine the minimum distance that the detonation wave must travel to build up the required duration. In actual field conditions, greater distances will be required to compensate for the motion of the overburden, since the motion of the overburden will decrease the duration.

Therefore, the next step in the development of this technique was to predict the effect of the motion of the overburden. The method used to make these predictions is described in appendix I. Figures 11 through 13 illustrate how to vary the duration to half pressure by varying the size of the flexible container, the weight of the overburden, and the distance from ignition for a 300-psi simulation. Curves similar to these for other overpressures may be constructed using the computer program in appendix I.

Up to this point, the simulation technique has been developed in theory with some verification under ideal laboratory conditions in the high-pressure shock tube. The next problem was to verify the simulation in large-scale

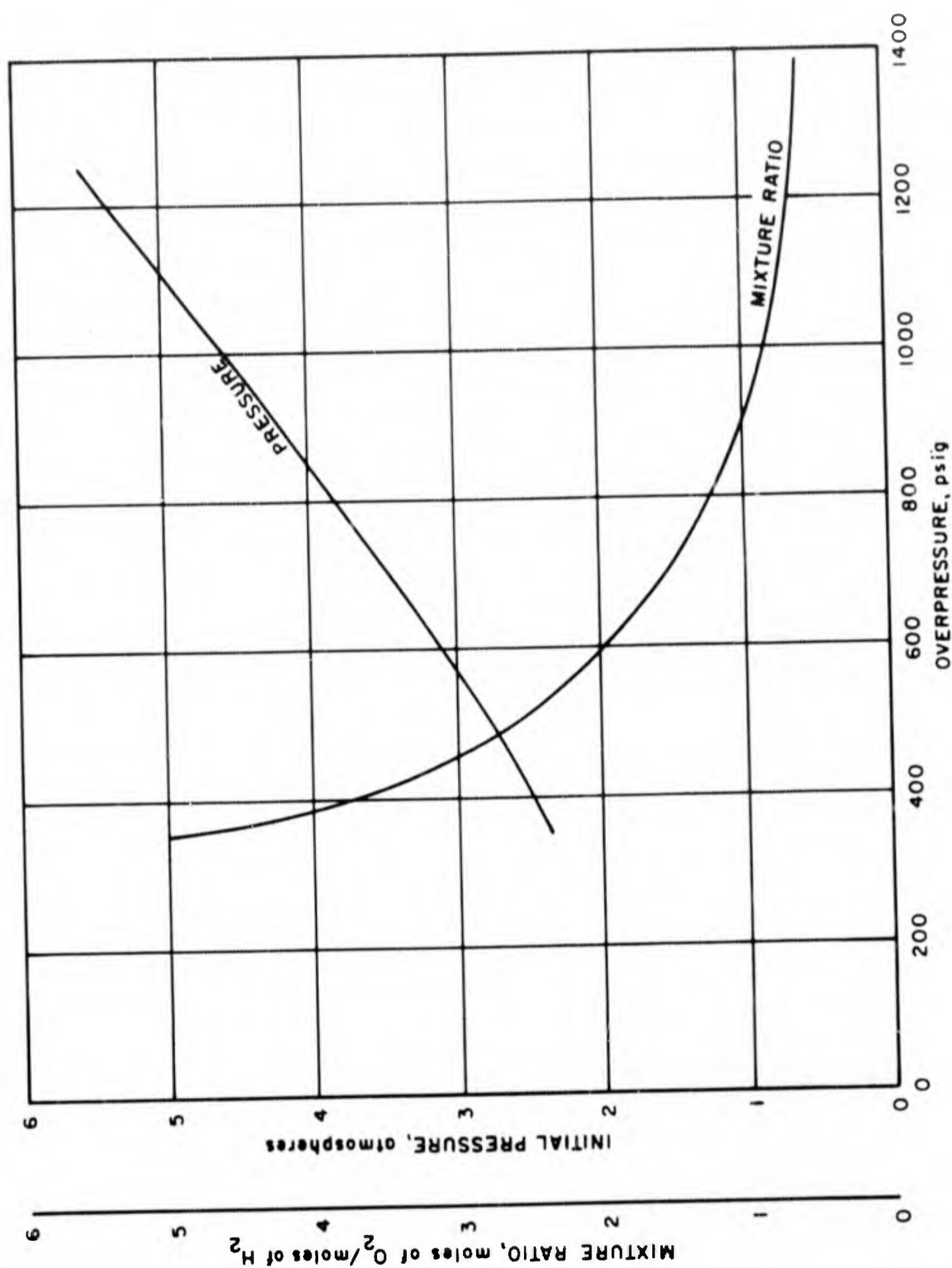


Figure 10. Initial Mixture Conditions Required to Simulate Air Shock Waves

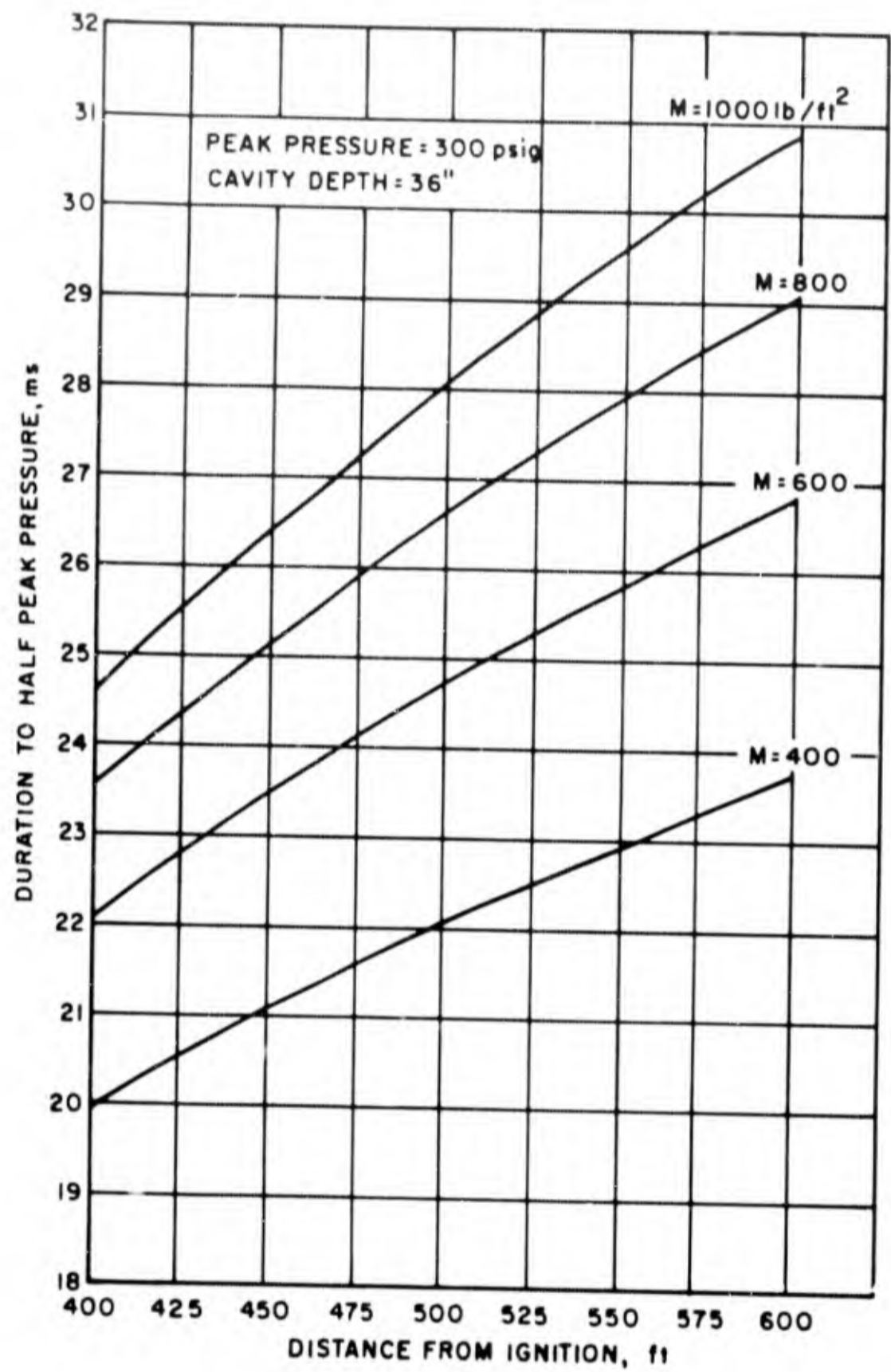


Figure 11. Duration to Half Peak Pressure--Peak Pressure = 300 psig, Cavity Depth = 36 inches

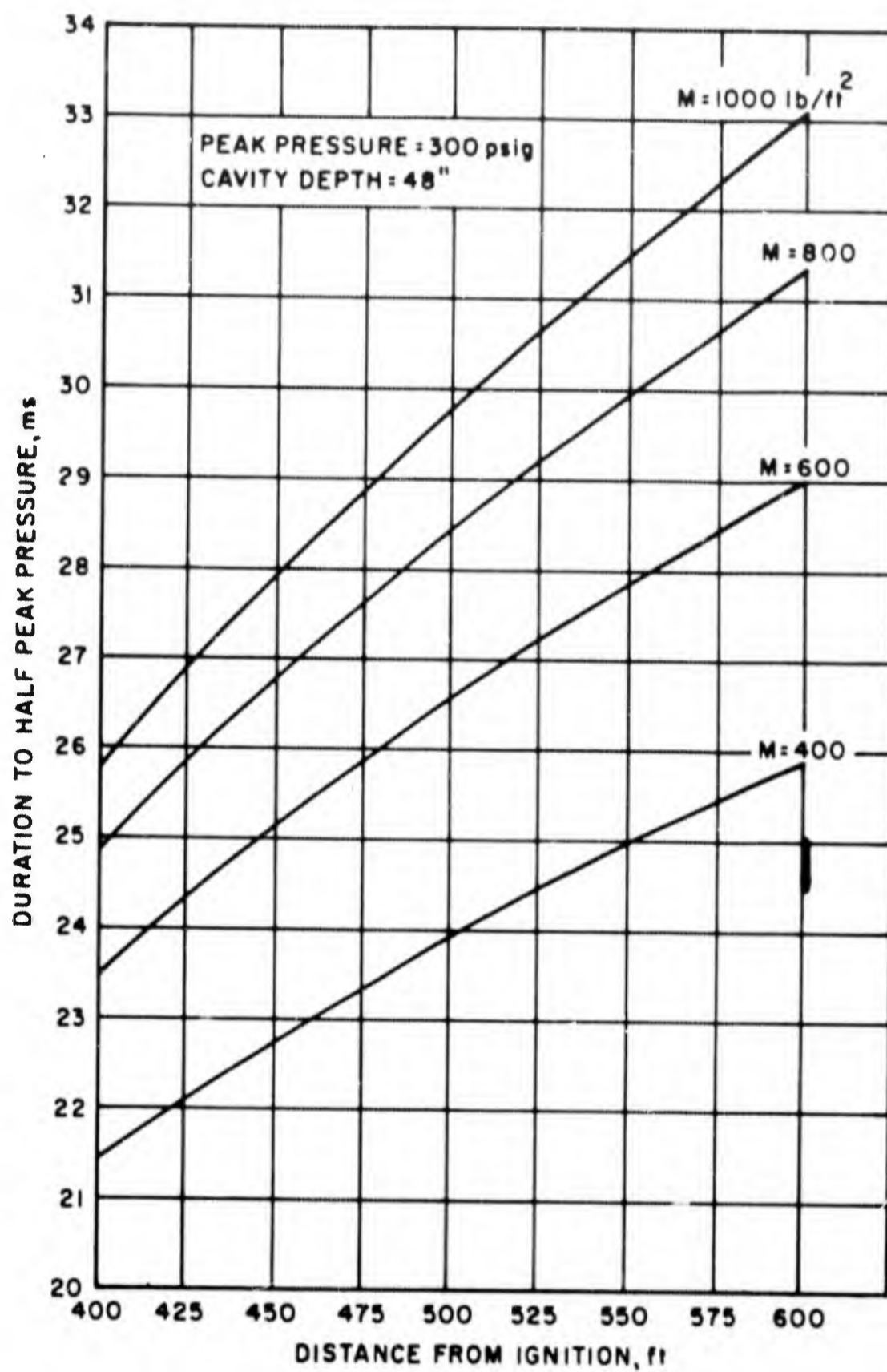


Figure 12. Duration to Half Peak Pressure--Peak Pressure = 300 psig, Cavity Depth = 48 inches

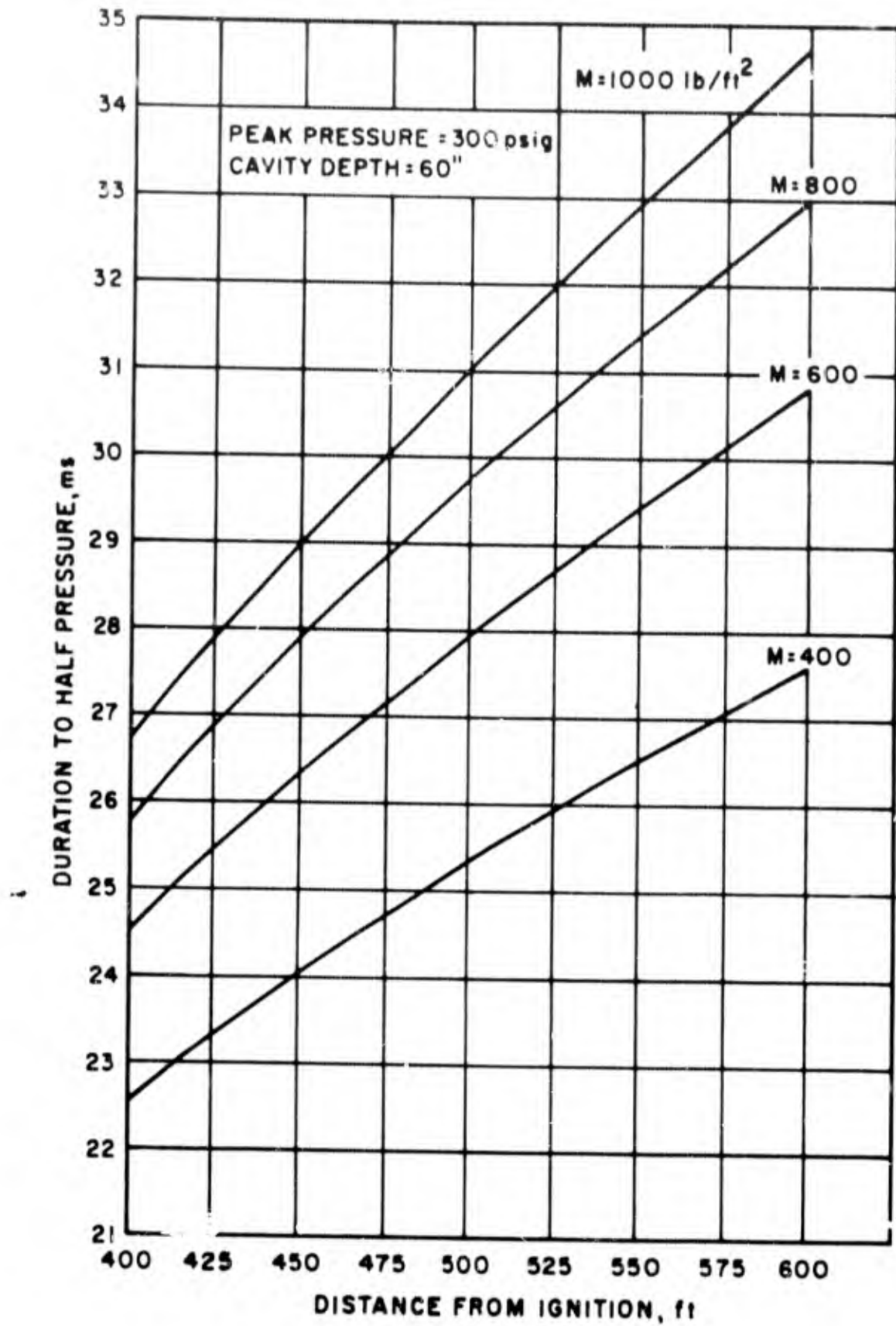


Figure 13. Duration to Half Peak Pressure--Peak Pressure = 300 psig, Cavity Depth = 60 inches

field tests. To do this the facility shown in figure 14 was constructed. A pit 20 feet x 40 feet in plan was dug and lined with a reinforced concrete retaining wall. The wall was 1 foot thick at the top and 7.5 feet thick at the base. The pit was 12 feet deep. A flexible container, or bag, is placed in the bottom of the facility and a waterproof cover is placed over the bag. Figure 15 is a photograph showing the facility with a bag in place. Next, the desired amount of overburden is placed over the waterproof cover. The bag is then filled with a detonable gas mixture and detonated along one end. The detonation wave moves through the bag and induces ground motions in the soil at the bottom of the pit that are similar to those motions caused by a traveling air shock. The gas in the bag is ignited by a 20-foot length of primacord with blasting caps placed at 2-foot centers. This amount of explosive was required to produce a detonation wave immediately. Tests in the shock tube showed that it would take more than 40 feet to form a stable detonation if a spark was used for ignition.

Since a two-atmosphere container had to be developed and was not available at the beginning of the project, a series of three low-pressure tests was initiated. Figure 10 shows that two atmospheres is the minimum initial pressure required to produce a 300-psig detonation wave with the correct air shock frontal velocity of 4,800 feet per second. The purpose of these three tests was to obtain a stable detonation, to obtain predictable pressures and velocities, and to obtain some experimental overburden data.

Since 6-mil polyethylene was readily available, three containers were fabricated using this material. Tests showed that these containers would hold only a one atmosphere mixture. The atmospheric pressure at the Air Force Shock Tube Facility was 12 psi on all three tests. A mixture with a three-to-one molar ratio of oxygen to hydrogen was selected for all three shots. This mixture ratio was calculated to produce a 150-psig overpressure (162 psia) detonation wave. The predicted velocity of 5,600 feet per second will be 60 percent too high to match an air shock with this pressure.

Figure 6 is a graph of the Hugoniot curve for this mixture. The curve was computed using a computer program developed at the Air Force Weapons Laboratory. This particular program considers only the dissociation in the products of water to hydrogen and oxygen. This is a valid assumption



Figure 14. Detonable Gas Facility

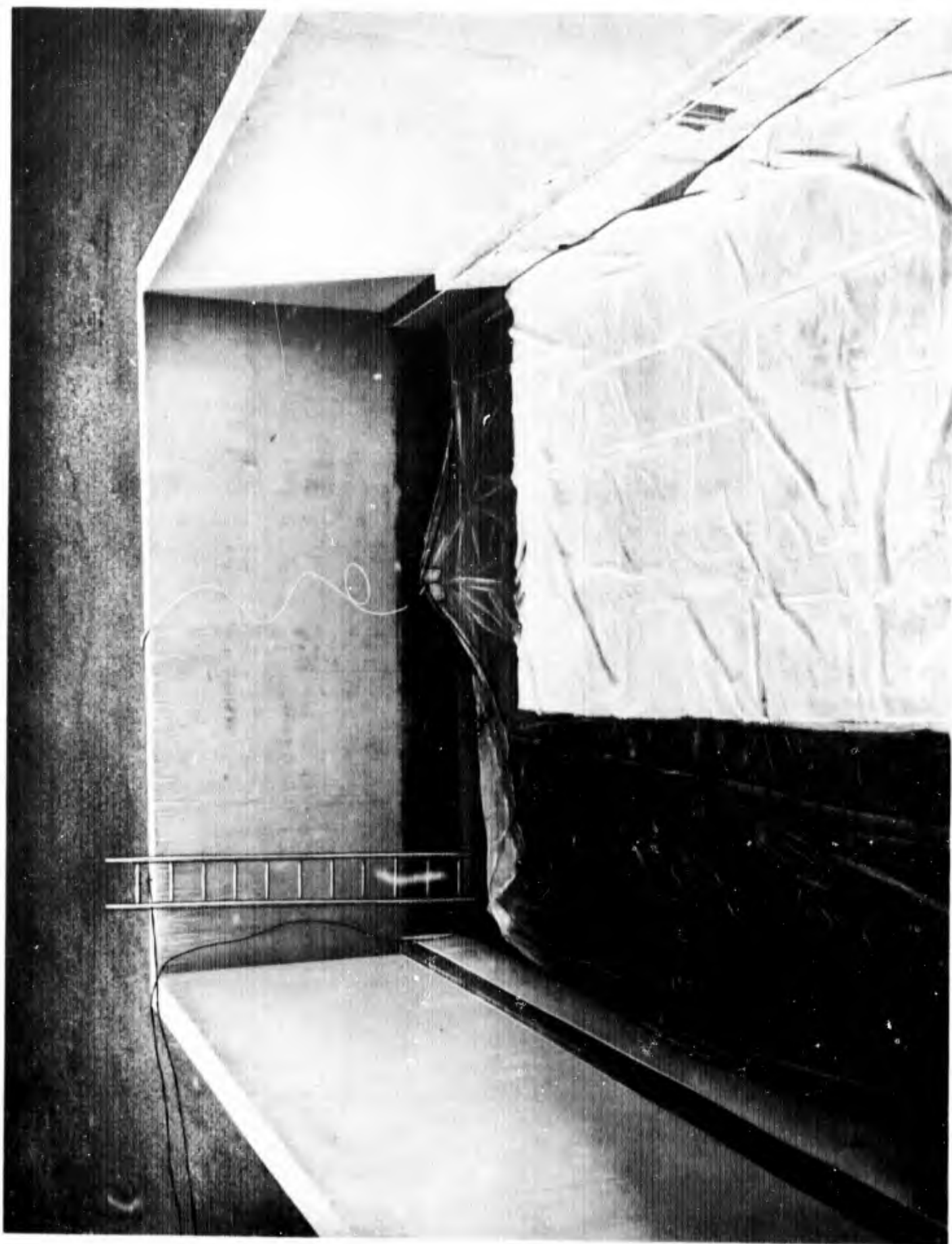


Figure 15. Detonable Gas Facility (Photograph)

at these lower detonation temperatures.

Figure 7 is a graph of the velocity versus pressure along the Hugoniot curve. It was hoped to determine the pressure variation from the fluctuations in velocity. The assumption was that all fluctuations in velocity correspond to pressures on the Hugoniot. This seemed to be a reasonable assumption since the Hugoniot represents a locus of end conditions that satisfy the conservation of energy and momentum along with the continuity equation. High-speed photography was used to observe the detonation wave front. Figure 16 is a series of detonation photographs taken during the second test. The framing rate was 1,000 frames per second. This framing rate is too slow to resolve the variations in detonation velocity; however, the average velocity of 5,520 feet per second taken from these photographs agrees well with the calculated velocity of 5,600 feet per second. Note that the detonation front is very plane.

Stable detonations were observed on all three tests. Excellent correlation was observed between the predicted pressures and velocities and the observed values. Table II illustrates this correlation. Surface pressure instrumentation was lost on test No. 2. However, some buried soil stress gages indicated an average pressure of 160 psia.

Surcharge data are available from the first test only. In this test, a lightweight polyethylene bag was used to contain the gas mixture. This type of bag cannot support an overburden; therefore, steel plates were placed on the rim of the facility and over the bag to support the surcharge. This arrangement formed a 2-foot-high cavity for the inflated bag. A waterproof liner was then placed over the steel plates and a 6.4-foot-deep water surcharge was filled in over the liner. Figure 17 shows the calculated durations to half pressure as a function of distance from ignition. The observed durations are plotted over this curve. There are too few data points to draw any definite conclusions. At 10 feet from ignition, the data bracket the theoretical curve. At 20 feet, the duration was short, and at 30 feet the duration was long. In addition to the spread in the data, the surcharge mass was great for the relatively short 40-foot travel distance. Therefore, the theoretical curve is nearly straight. More data for different amounts of overburden must be gathered before any firm conclusions can be reached.

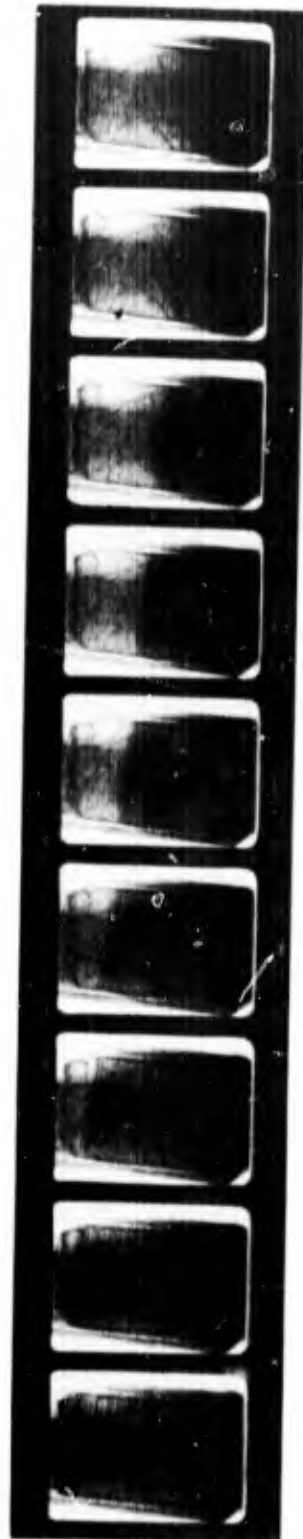


Figure 16. Detonation Wave Photography

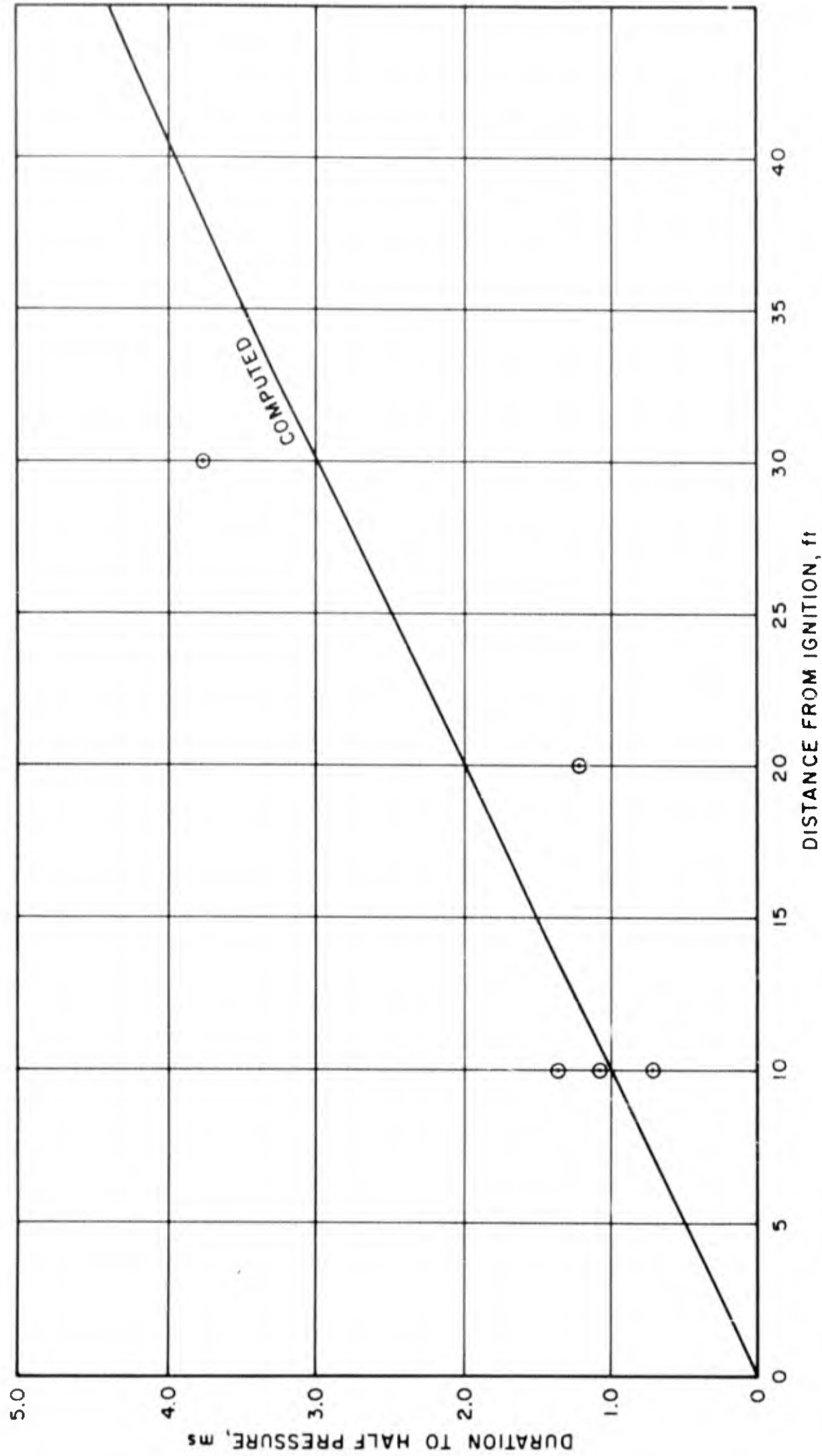


Figure 17. Duration to Half Pressure--Test No. 1

In each observed pressure-time history there was good correlation between the predicted and the observed wave shape. Figure 18 illustrates the correlation observed in the first test on gage No. 1.

Table II

RESULTS FROM DETONATION TESTS

Test	Pressure (psia)		Velocity (fps)	
	Calculated	Observed	Calculated	Observed
1	162	162	5,600	5,625
2	162	(not observed)	5,600	5,520
3	162	180	5,600	5,820

As stated earlier, more overburden data are needed to accurately predict durations. It was planned to obtain such data from a series of high-pressure tests; however, a satisfactory flexible container to hold pressures greater than two atmospheres was never developed. Figure 19 illustrates the container that was tested. This bag was manufactured of nylon-reinforced neoprene. In the first test using this container, the container ruptured under the two-atmosphere pressure. Fortunately, the bag was being filled with oxygen to its design pressure when it ruptured. The second container began leaking so badly it had to be detonated prematurely, and there was not time for diffusion or adequate mixing. Shock-tube tests showed that at least two hours is required for adequate mixing under ideal conditions. High-pressure tests, which require a two-atmosphere container, were never performed utilizing the detonable gas method since by this time the primacord technique had been developed and appeared to be the more worthy simulation technique. However, the detonation technique would be an excellent simulation if an economical container could be fabricated. A flexible sheet metal container was designed to hold the two-atmosphere initial pressures required for a simulation, but this design was never tested. Another serious drawback to this simulation technique is the requirement for a very large facility. This drawback can be quickly verified using the data presented in figures 11 through 13.

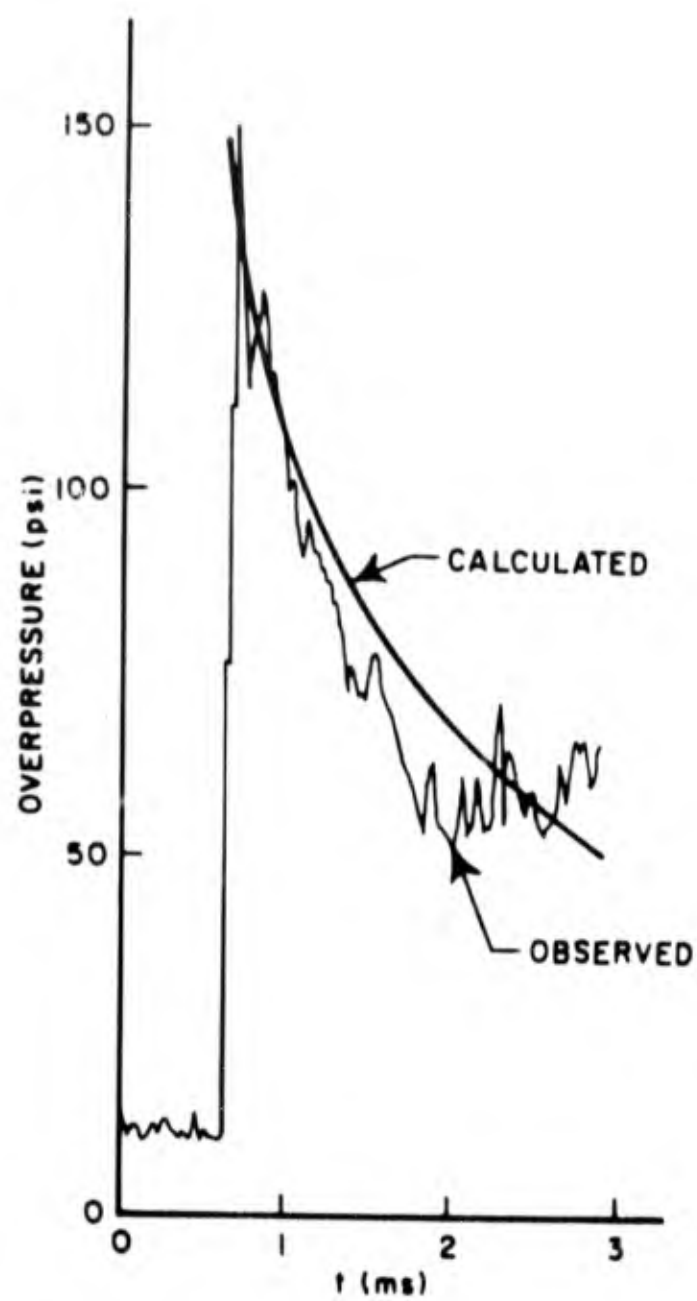


Figure 18. Test No. 1 Pressure Record

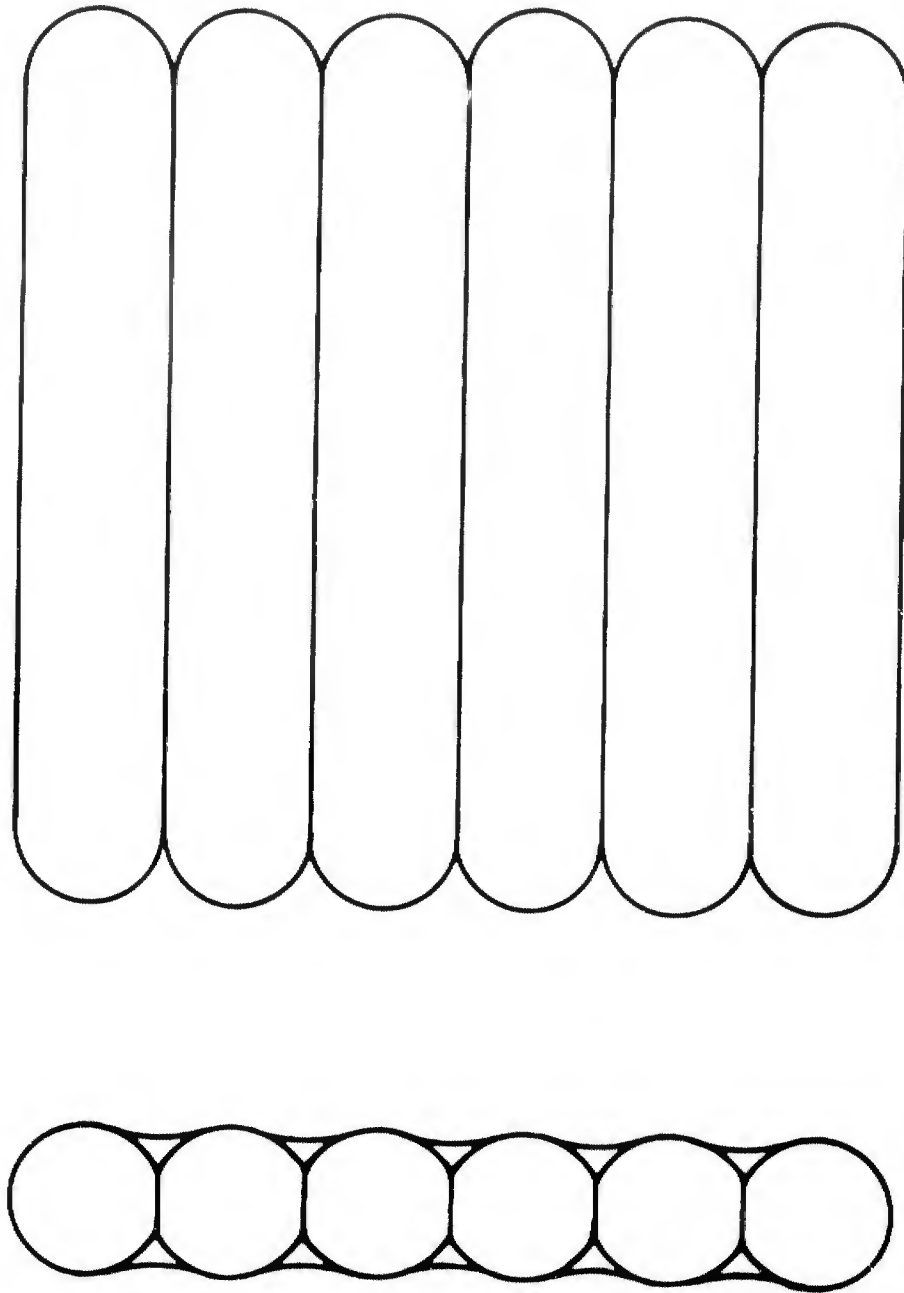


Figure 19. Two-Atmosphere Container

SECTION V

PRIMACORD SIMULATION TECHNIQUE

The concept behind the primacord technique is quite simple. As shown in figure 20, a length of primacord is suspended in a buried detonation cavity. The weave angle θ is selected so that

$$\sin \theta = \frac{U}{D} \quad (10)$$

where

U = desired frontal velocity

$D = 21,000$ feet per second = primacord detonation velocity

Primacord woven at this angle should give the correct frontal velocity. The peak pressure is defined after all of the small transient shocks have died out and the cavity has come to thermal equilibrium. The overburden then begins to move upward and causes the cavity to expand. The gases expand adiabatically in the cavity, which causes the pressure to drop. The cavity depth and the overburden mass may be adjusted to simulate the pressure decay. the method for computing the overburden motion is illustrated in appendix I.

The desired peak pressure is computed by considering the cavity to be an insulated, fixed volume. The energy released from the burning primacord is then assumed to be added isentropically to the fixed volume and the peak pressure computed. Figure 21 (from reference 5) illustrates the computed peak pressure versus the loading density.

The computed frontal velocity is shown in figure 22. These calculations were made using equation 10, assuming the primacord burning rate to be 21,000 feet per second. The manufacturer of the primacord recommended this value for the burning velocity.

The results of overburden calculations are presented in figures 23 through 27. The technique for computing these displacements is presented in appendix I. The ratio of specific heats, γ , was assumed to be equal to 1.3 for all cases, based on work presented in reference 5.

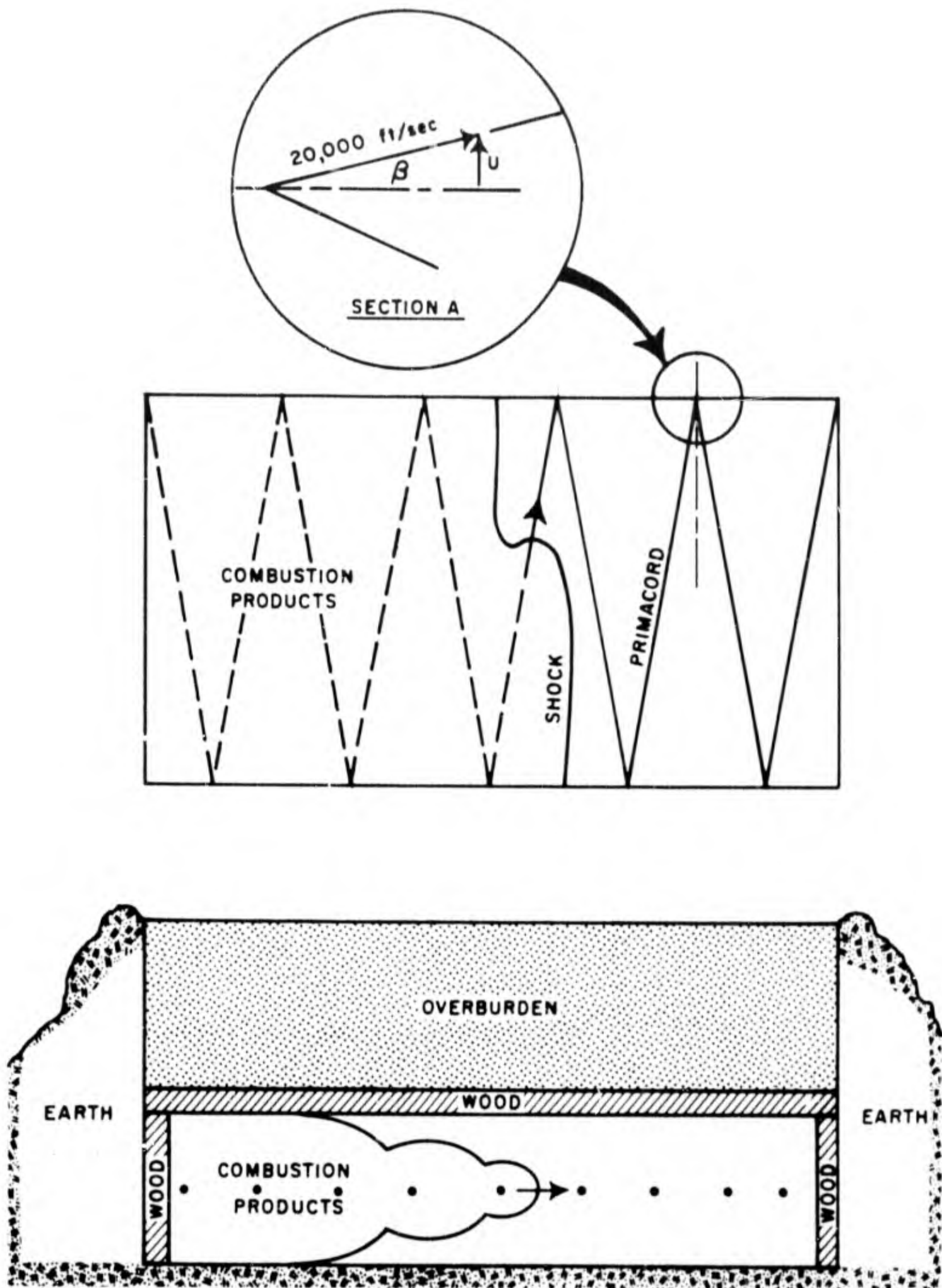


Figure 20. Primacord Simulation Technique

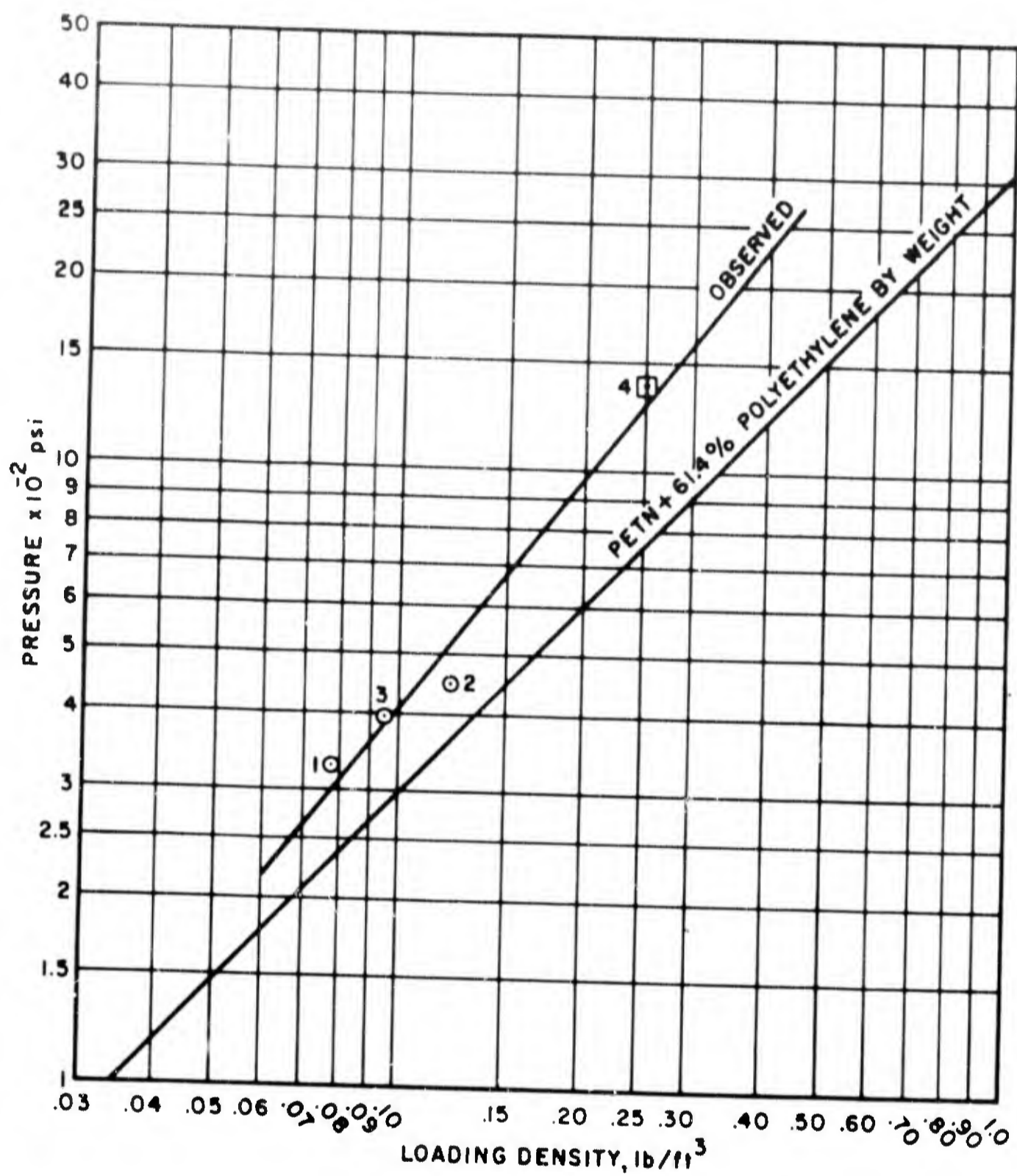


Figure 21. Peak Overpressure versus Loading Density

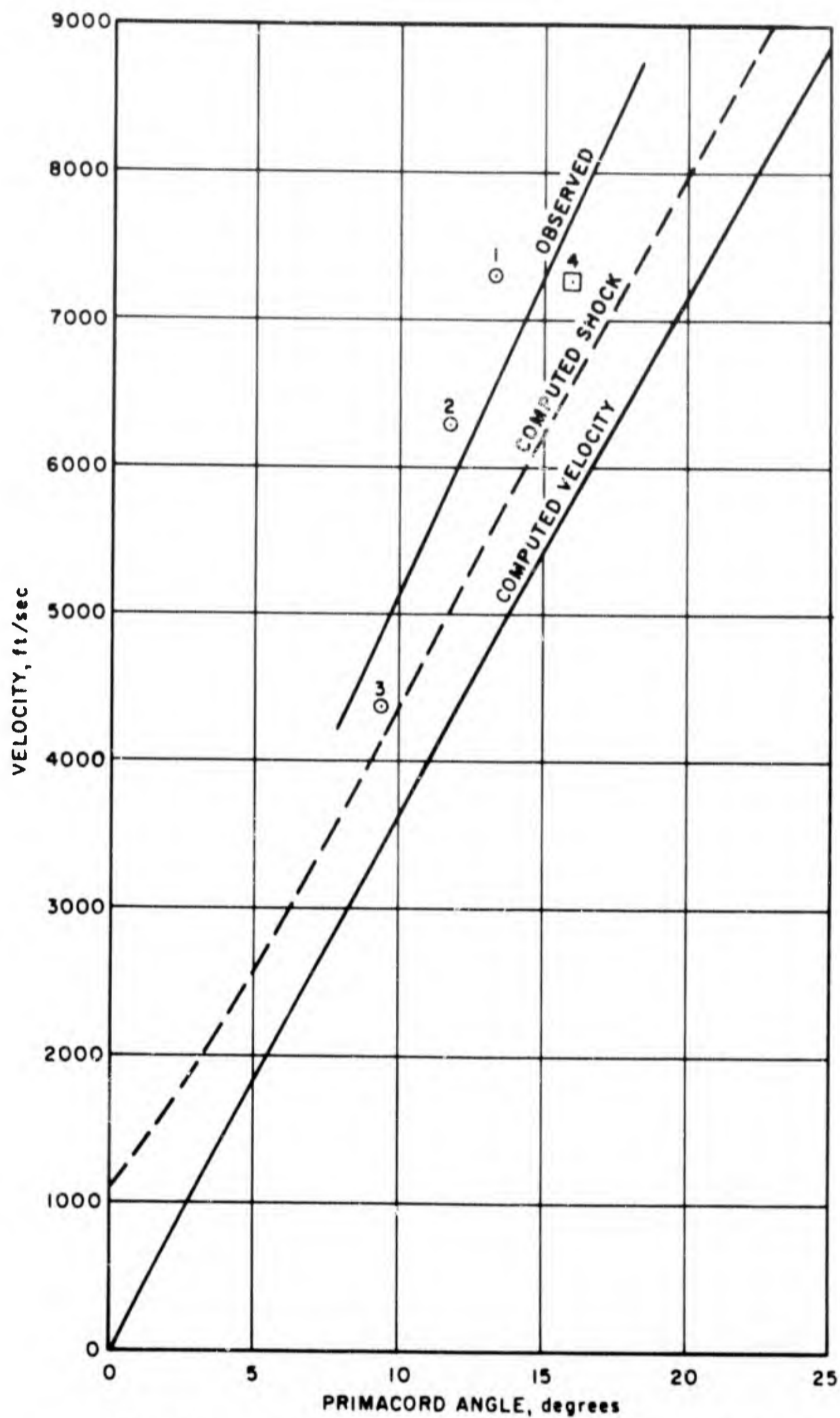


Figure 22. Shock Velocity versus Primacord Weave Angle

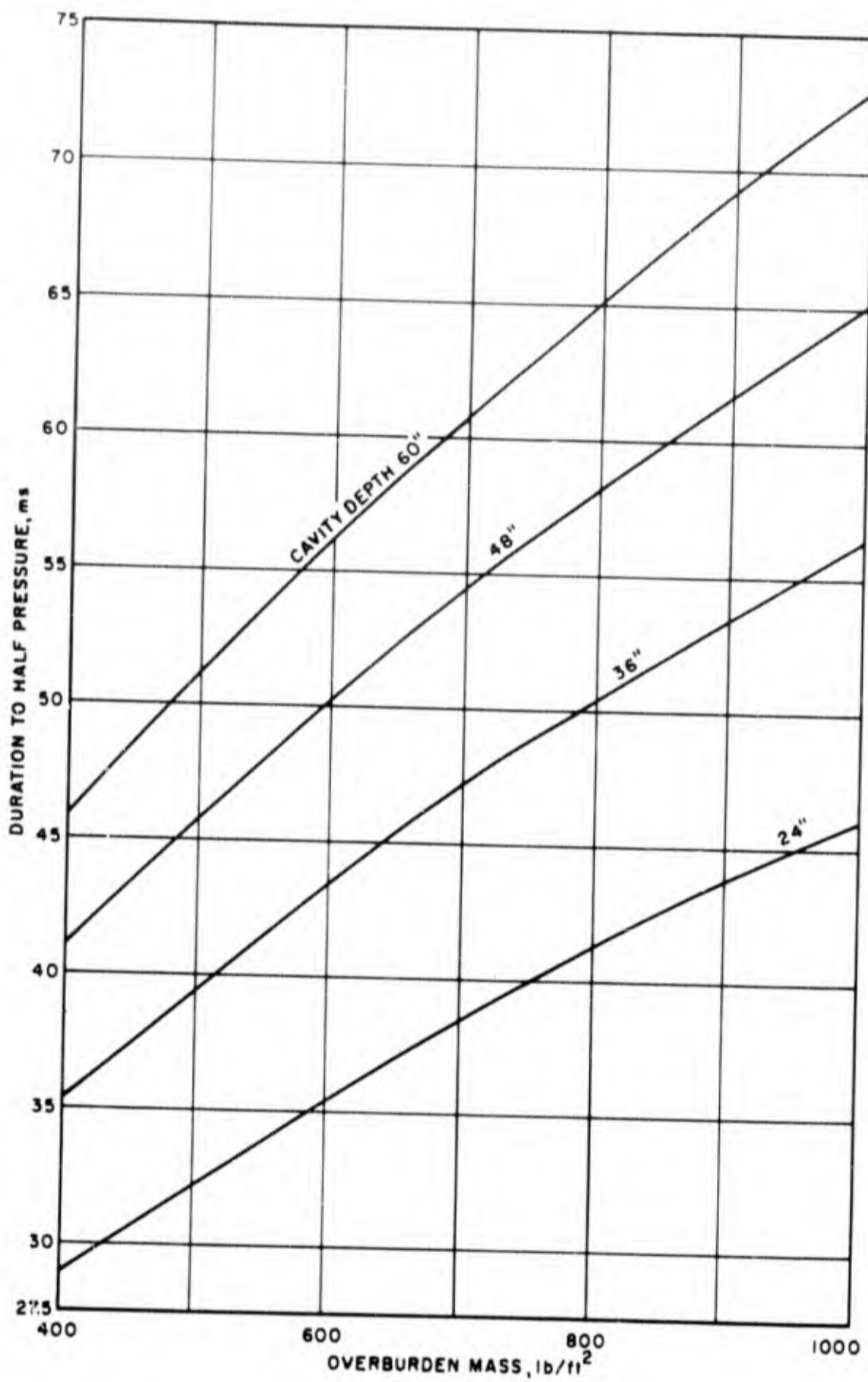


Figure 23. Duration to Half Peak Pressure--Peak Pressure = 300 psig

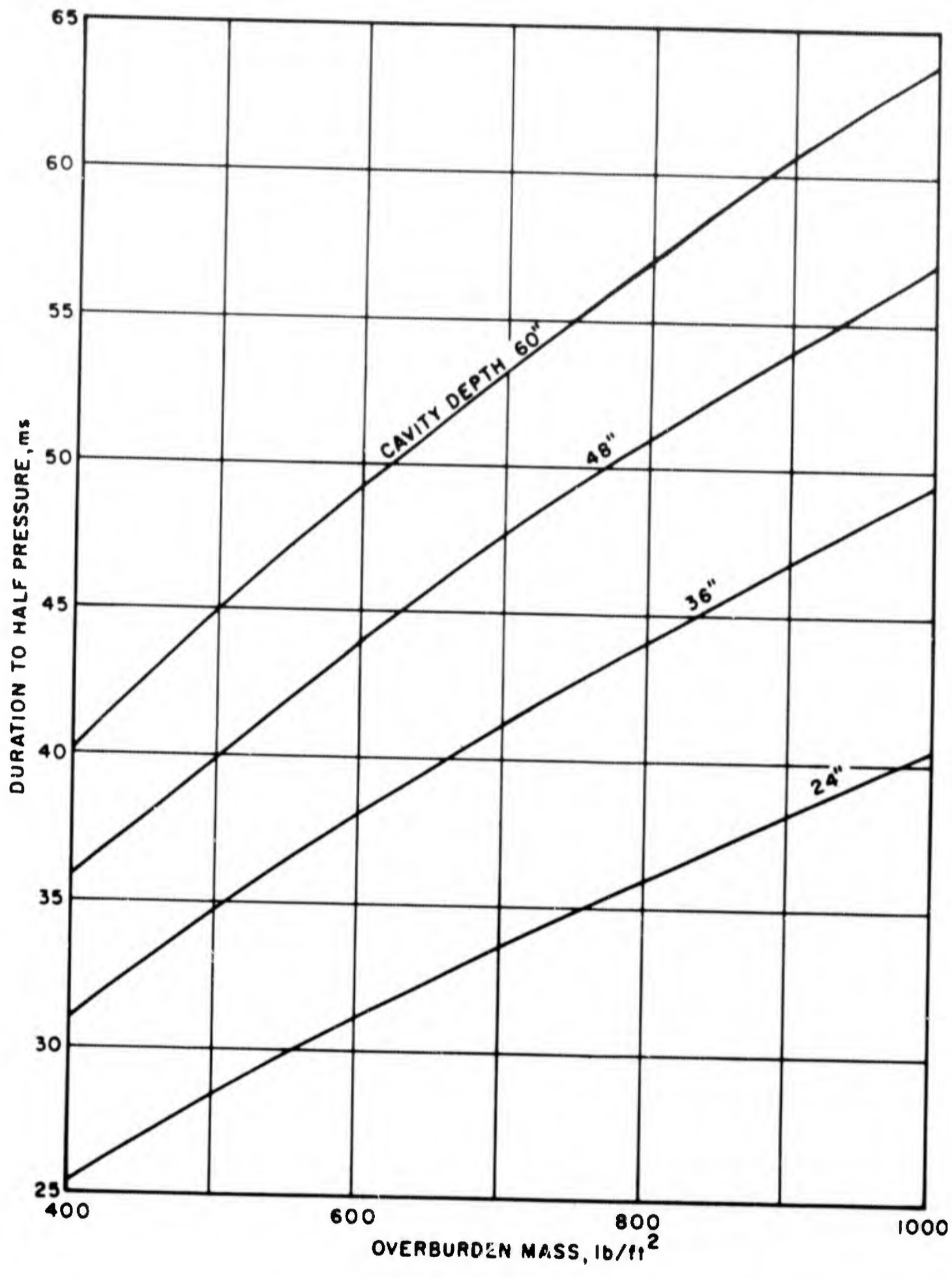


Figure 24. Duration to Half Peak Pressure--Peak Pressure = 400 psig

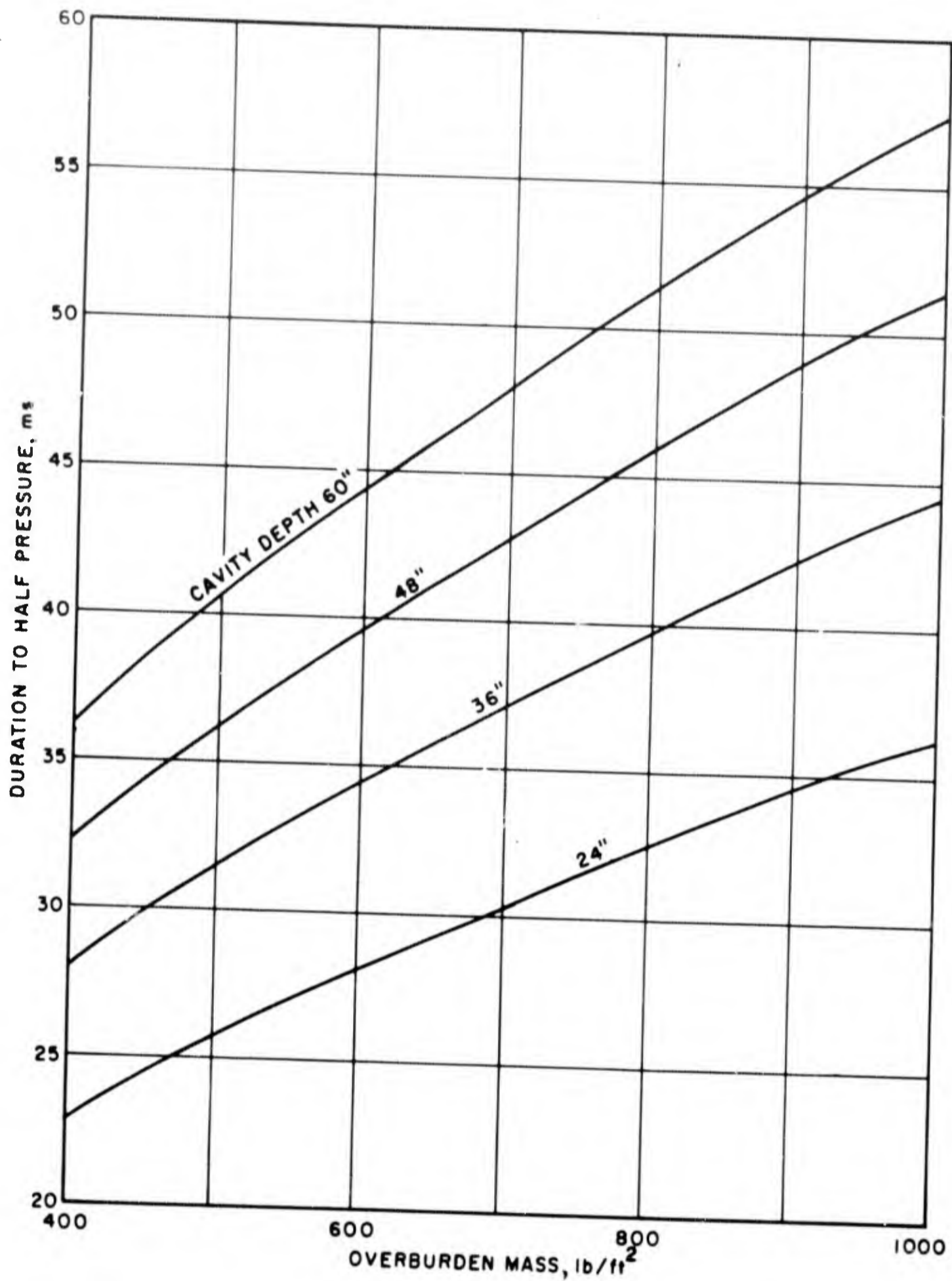


Figure 25. Duration to Half Peak Pressure--Peak Pressure = 500 psig

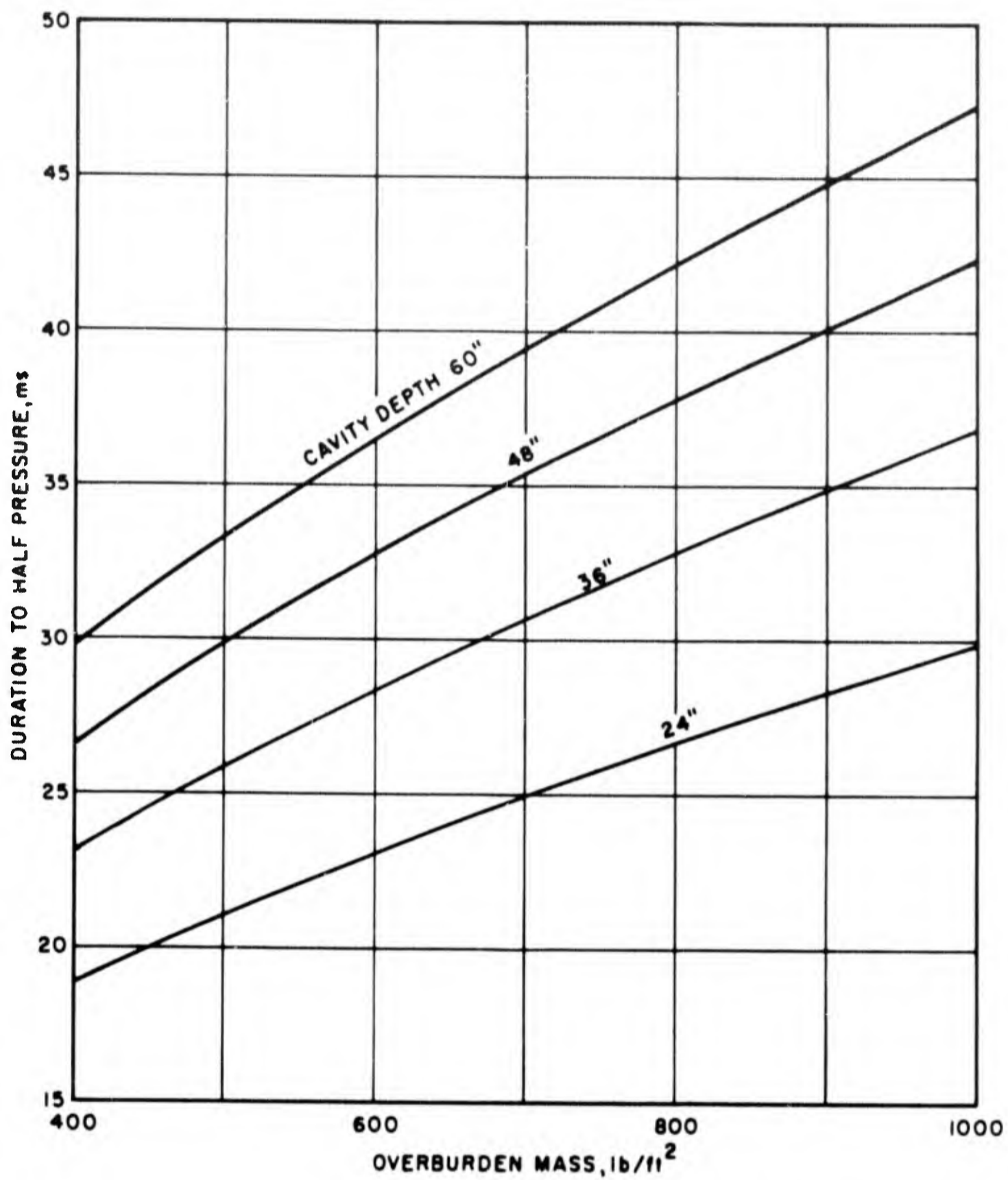


Figure 26. Duration to Half Peak Pressure--Peak Pressure = 750 psig

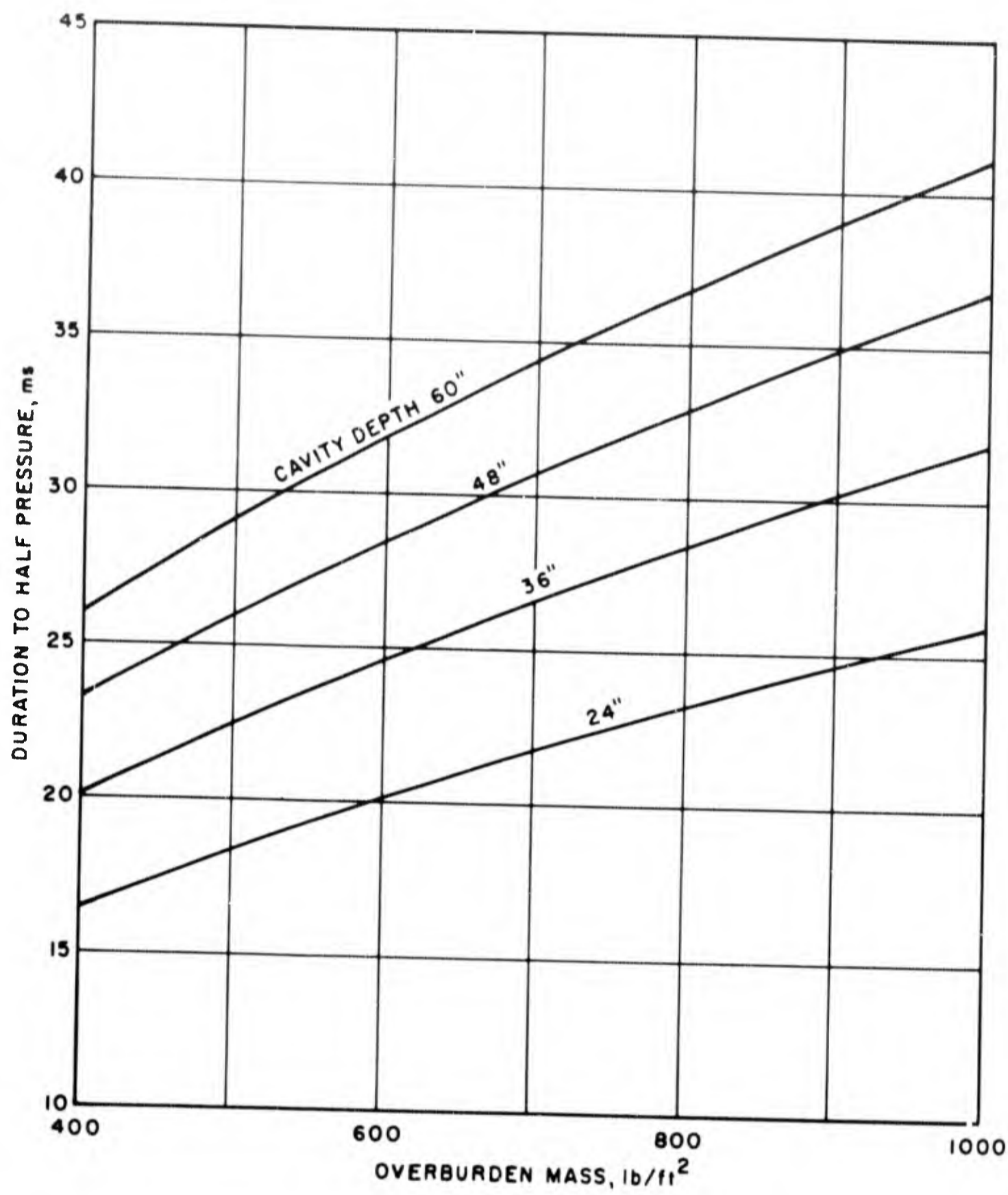


Figure 27. Duration to Half Peak Pressure-Peak Pressure = 1,000 psig

The next step in the development of the primacord technique was to field-test the theory. The field-test series consisted of four experiments. The first experiment was performed in the facility illustrated in figures 14 and 15. Figure 28 presents details of the first experiment. The primacord racks were placed in the center of a 2-foot cavity and are supported by the columns used to support the floor of the overburden. A 7.33-foot water overburden, which is equivalent to 458 pounds per square foot, was placed over the floor. A loading density of 0.0943 lb of PETN/ft³ and a primacord weave angle, β , of 13.2 degrees was selected. Reference 5 served as a basis for the selection of these values, which were intended to produce a 300-psi overpressure shock wave.

The second primacord test was similar to the first test in that it was performed in the same facility with similar construction techniques. However, a 500-lb/ft² earth overburden was used as surcharge over a 3-foot cavity. In this experiment, a loading density of 0.1215 lb of PETN/ft³ and a weave angle of 11.78 degrees were chosen.

Figure 29 illustrates the configuration of the third test which was conducted in an earthen embankment. This embankment enclosed a 20 foot x 40 foot test area. In this experiment, a loading density of 0.0778 lb of PETN/ft³, 500-lb/ft² overburden, and a weave angle of 9.34 degrees were used.

The fourth high explosive test was conducted by the Air Force Shock Tube Facility in a facility similar to the one described in test No. 3. A 400-lb/ft² earth surcharge was used, the cavity depth was 3 feet, and double primacord racks were used to accommodate the loading density of 0.25 lb of PETN/ft³ with a weave angle of 15.9 degrees.

Table III and figures 21 and 22 present the pressure and the velocity results for the four experiments. The correlation between the simple theory and the results is unacceptable; both pressures and velocities are too high. Several explanations can be offered. The most reasonable argument is that the combustion products may be compared with the analogy of a piston in a shock tube, which is illustrated in figure 30. The piston is shown moving at a constant velocity, u . A shock is produced and moves out ahead of the piston at a constant velocity, U . The piston velocity, u , will correspond to the particle velocity behind the shock. Considering the old computed

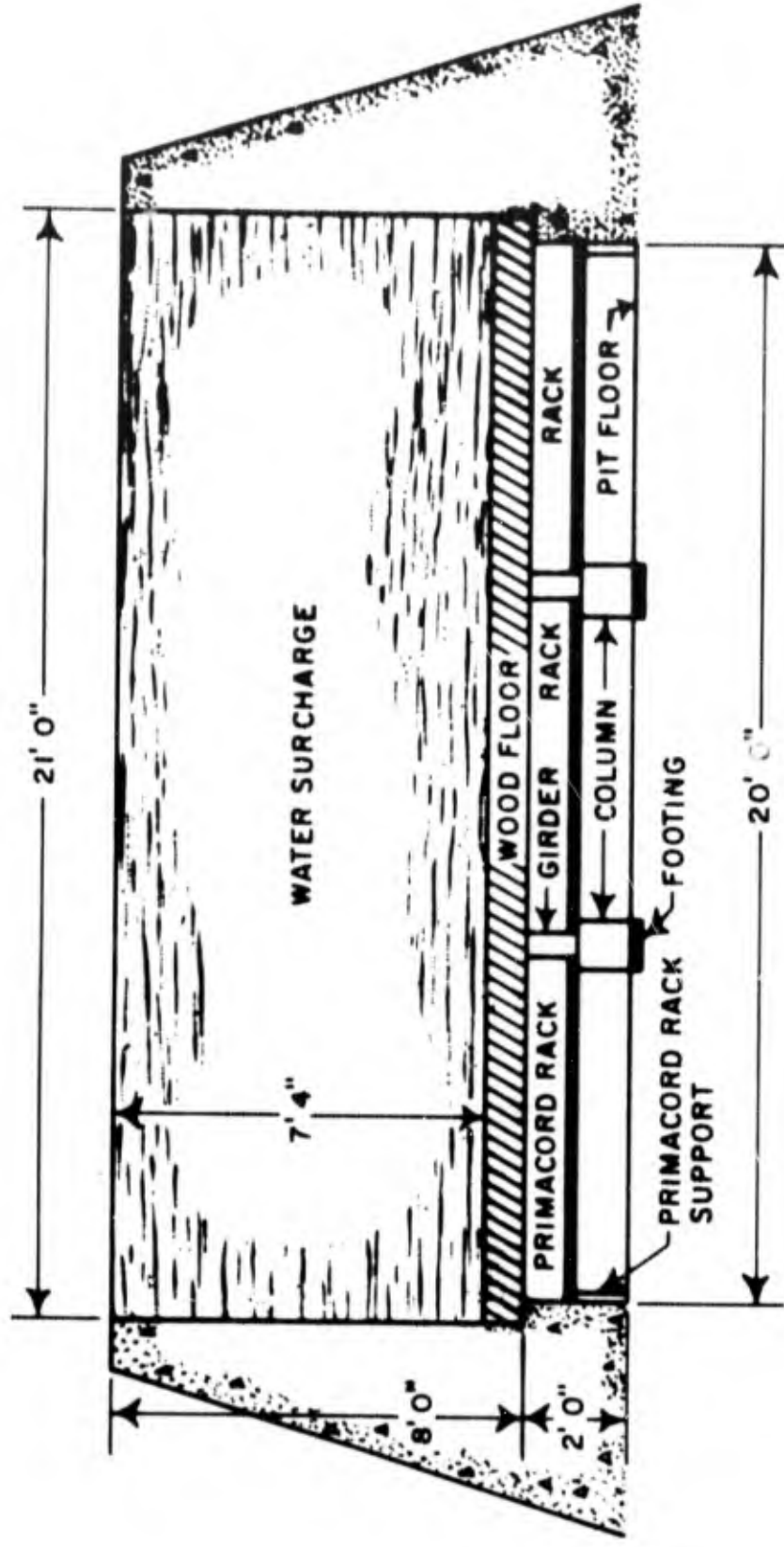


Figure 28. Primacord Experiment No. 1

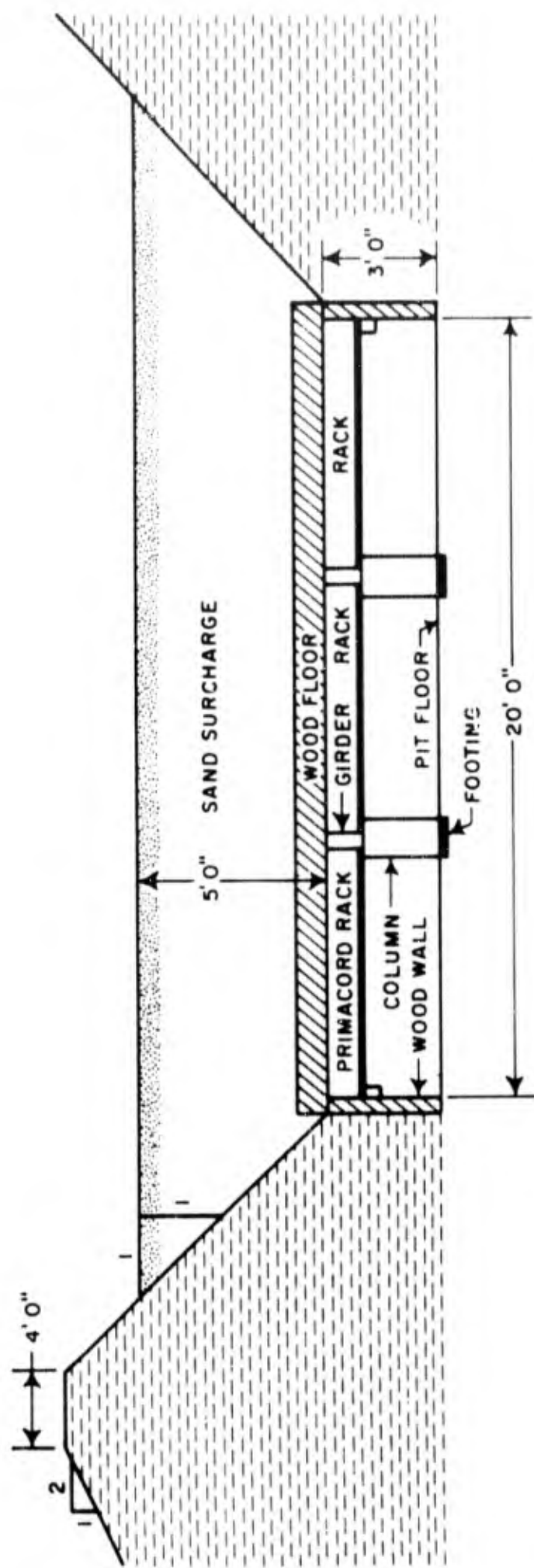


Figure 29. Primacord Experiment No. 3

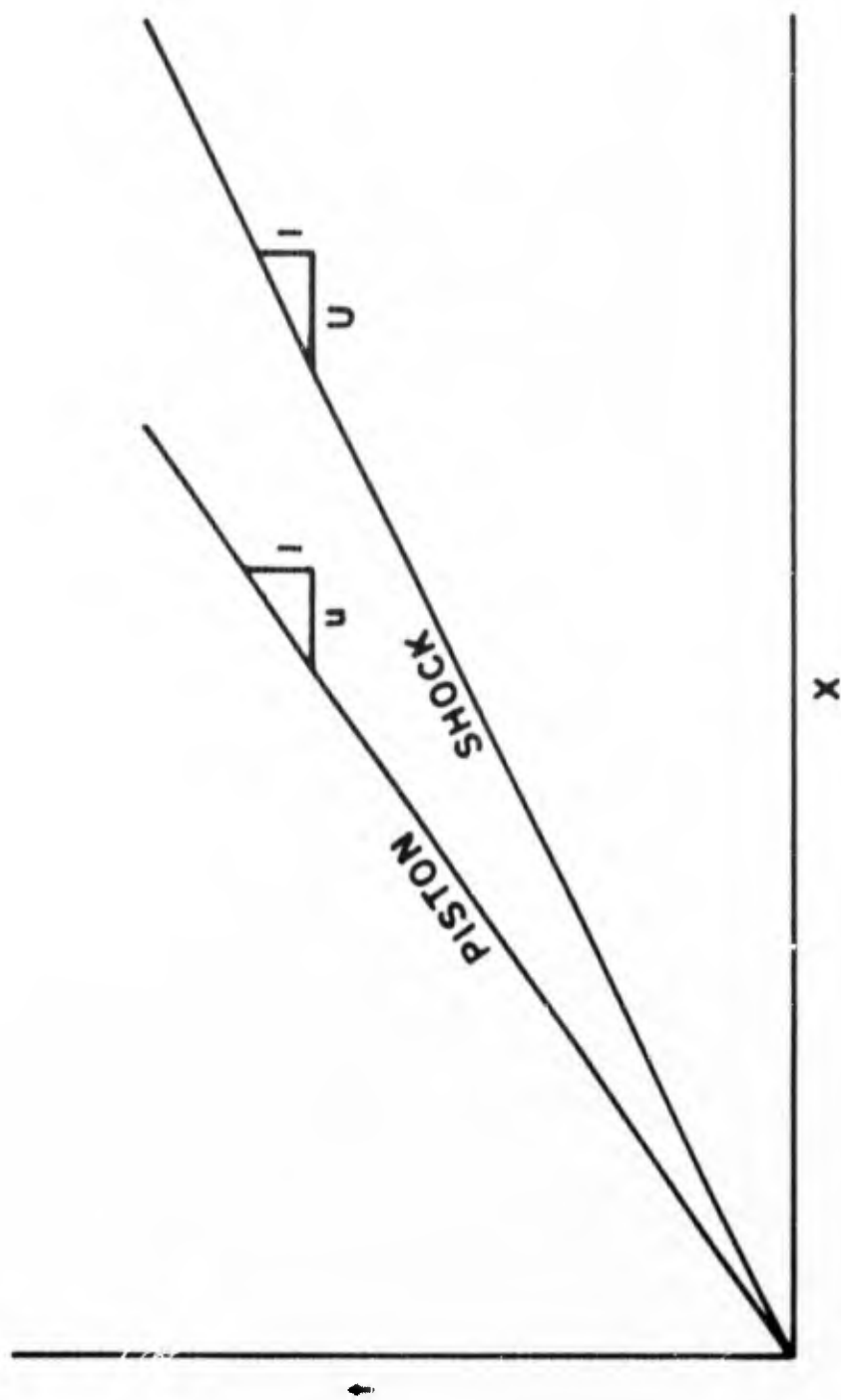


Figure 30. Shock-Tube Piston Analogy

BLANK PAGE

Table III
RESULTS FROM PRIMACORD TESTS

Test numbers	1	2	3	4
Loading density (lb of PETN/ft ³)	0.0943	0.1215	0.0778	0.2500
Primacord angle (degrees)	13.20	11.75	9.34	15.90
Cavity depth (feet)	2	3	3	3
Overburden (lb/ft ²)	458	500	500	400
Pressure (psig)	395	450	325	1,375
Shock velocity (ft/sec)	7,300	6,330	4,330	7,280
Duration to half peak pressure (milliseconds)	7.8	14.8	---	7.5

frontal velocity to be the velocity of formation of combustion products which, in turn, represents the piston in figure 31, a new shock frontal velocity was computed. The results of this computation are labeled the COMPUTED SHOCK in figure 22. There is still a large discrepancy between theory and observation. A possible explanation for this discrepancy is that a small intense shock is produced as each section of primacord detonates. This shock may be propagating rapidly behind the main shock. Each small shock will reinforce the main shock when it overtakes the main shock, which will cause a corresponding increase in the frontal velocity.

An examination of figure 31 provides some basis for the above hypothesis. This is a typical pressure-time history from the first test in which the minor shocks are clearly seen. The reinforcement of the main shock by the minor shocks builds up a natural pressure decay that is independent of the overburden motion. Since a significant portion of the blast wave impulse is

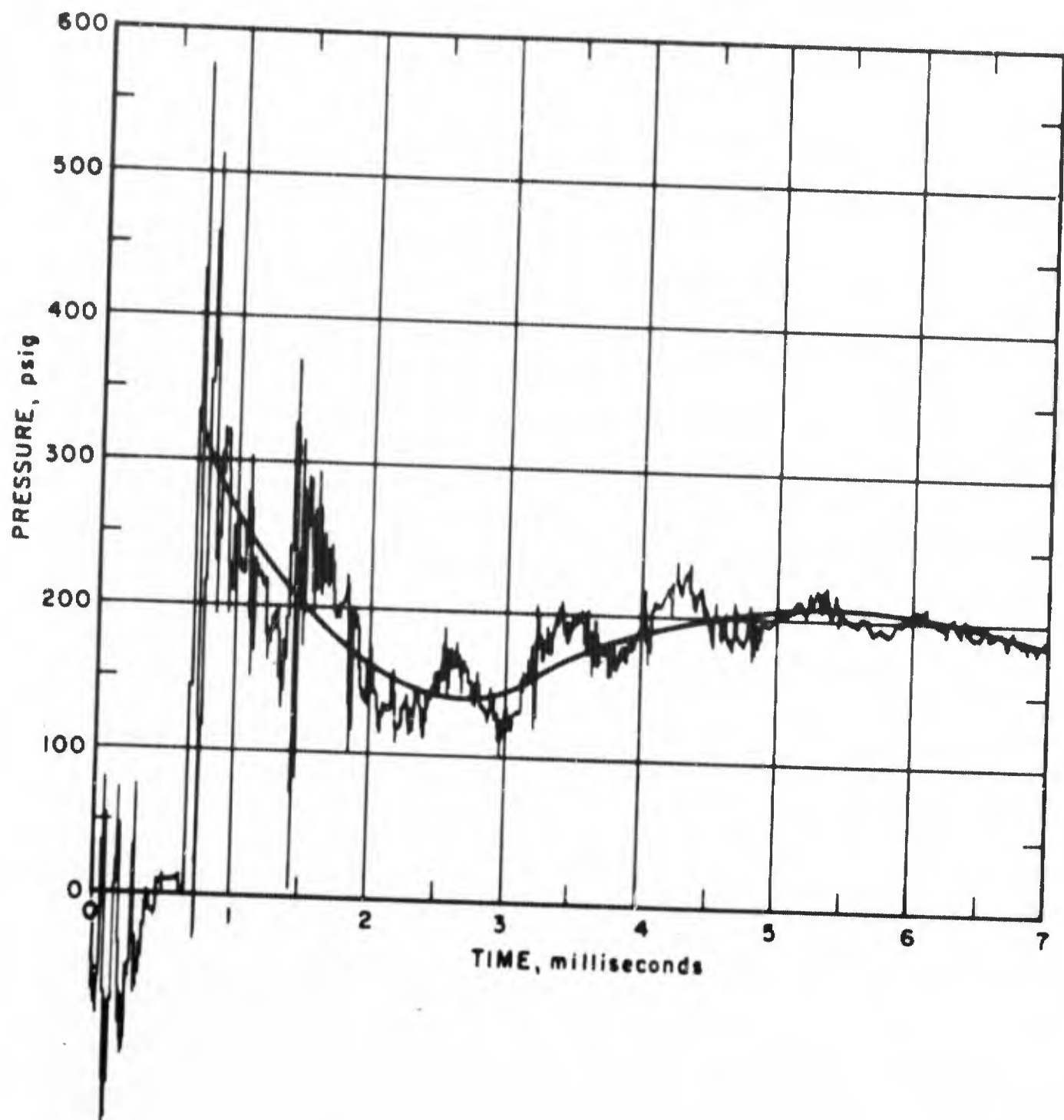


Figure 31. Typical Pressure Trace

is represented in the early part of the pressure pulse, this portion of the pulse cannot be ignored. The pressure was calculated for small time increments by conserving the impulse during the increment. Next, a least-square fit was made using these pressure points. This was done for each pressure history, and the average was assumed to represent the pressure obtained in a given experiment.

The increase in pressure followed by a slow decay was observed in all pressure-time histories. This may represent the arrival of the combustion products; however, this phenomenon lagged the shock front by approximately the same time on all records. If this hump represents the combustion products, the lag time should increase with the propagation distance.

In both figures 21 and 22 a least-square fit was made with all the data points. These fits are labeled OBSERVED in both figures. These two lines represent the revised predicted values that may be used in future tests.

Duration predictions were revised by recomputing the overburden displacement using the observed average pressure for each test. These new values were then compared with observed values. Table IV illustrates this comparison.

Table IV
EFFECT OF CAVITY DEPTH ON DURATION

Cavity depth (feet)	Overburden (lb/ft ²)	Pressure (psig)	Ratio of observed duration to computed duration to half pressure
2	458	395	0.279
3	500	450	0.444
3	400	1,375	0.433

Two tests were made with a 3-foot cavity at two widely separated pressure levels. Also, the variation of the mass of the overburden between the two tests was 20 percent. The ratio of observed duration to computed duration is nearly constant. Assuming that the ratio of observed to computed durations will be insensitive to pressure and overburden for the 2-foot cavity, the variation in this ratio between the two cavity depths was assumed to be a

function of the cavity depth only. The ratio of observed duration to computed duration is about half that observed in a 3-foot cavity. Figure 32 illustrates the possible effect of varying the cavity depth. There is no real justification for extrapolating the curve from the two known data points; additional data are required. The slope of the curve is forced to decrease since observed durations are not likely to be larger than the computed durations. Therefore, it is recommended that the values for duration given in figures 23 through 27 be adjusted as indicated in figure 32.

More data are required before all variables which affect the primacord simulation technique can be assessed. However, some reasonable predictions may be made with the available data. The recommended procedure for designing a particular simulation is to first select the loading density and the weave angle using the curves labeled OBSERVED in figures 21 and 22. Next, the cavity depth and the overburden mass are selected from figures 23 through 27. Values given in these curves should then be corrected using figure 32.

This simulation technique will duplicate the shock pressure and the shock velocity over a point. The minor shocks are smoothed out after traveling a short distance in the earth. In the configurations tested, there is no decay with distance of peak overpressure, shock velocity, or impulse. There is a possibility that by varying the loading density, the weave angle, and the overburden with length, the decay of the pressure, velocity, and impulse might be simulated. As with the detonable gas technique, particle velocities and accelerations in the earth will reasonably approximate those produced by a nuclear explosion. The displacements will be small since the entire impulse from a nuclear detonation cannot be duplicated.

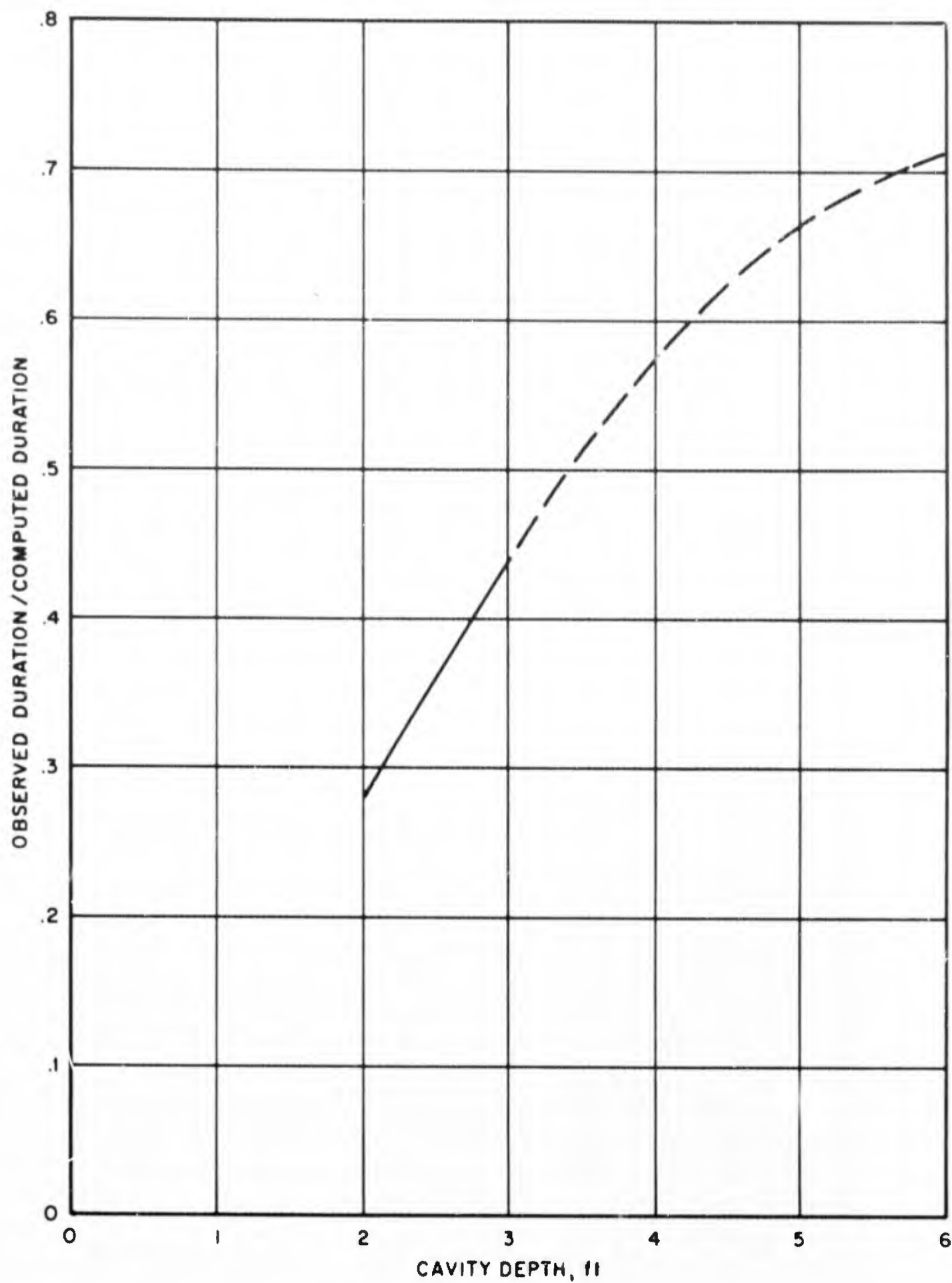


Figure 32. Effect of Cavity Depth

SECTION VI

CONCLUSIONS

Both techniques will produce adequate simulation of the air-blast-induced ground motions from a large nuclear weapon. However, the detonable gas technique requires a flexible container that will hold a two-atmosphere mixture. This is an extremely difficult design problem and will be expensive. Also, the detonable gas technique requires a much larger facility than does the primacord technique. The primacord technique is safer; mixtures of hydrogen and oxygen are extremely unstable and relatively dangerous to handle. Finally, the primacord technique is the more flexible of the two methods. A wider range of peak overpressures can be produced and the correct associated shock velocities are more easily provided. In addition, it appears feasible to generate an air-blast wave in which peak overpressure, shock velocity, and impulse decay with distance using the primacord technique, if such be deemed necessary.

APPENDIX I

DURATION CALCULATIONS

In both the detonable gas and the primacord simulation techniques, the motion of the overburden greatly influences the duration of the pressure pulse. This motion causes the cavity to expand with a resulting decrease in pressure. If the expansion due to the increase in cavity volume is considered to be isentropic, the following expression may be derived for the resulting pressure:

$$p_o V_o^\gamma = p V^\gamma \quad (11)$$

p_o = peak equilibrium overpressure

γ = ratio of specific heats of the explosion products

P = pressure in cavity at some time, t , after detonation

$$V_o = x_o dA = \text{initial volume of cavity} \quad (12)$$

dA = elemental area

x_o = initial cavity depth

$V = x dA$ = volume of cavity at some time, t

$$P_o (x_o dA)^\gamma = p (x dA)^\gamma \quad (13)$$

x = cavity depth at some time, t , after detonation

$$p(x) = p_o \left(\frac{x_o}{x} \right)^{-\gamma} \quad (14)$$

To determine the motion of the overburden, the equilibrium equations were applied to an elemental volume. Figure 33 illustrates the force acting upon this volume.

$$F = M \frac{d^2 x}{dt^2} \quad (15)$$

$$p(x) - a - Mg = M \frac{d^2 x}{dt^2} \quad (16)$$

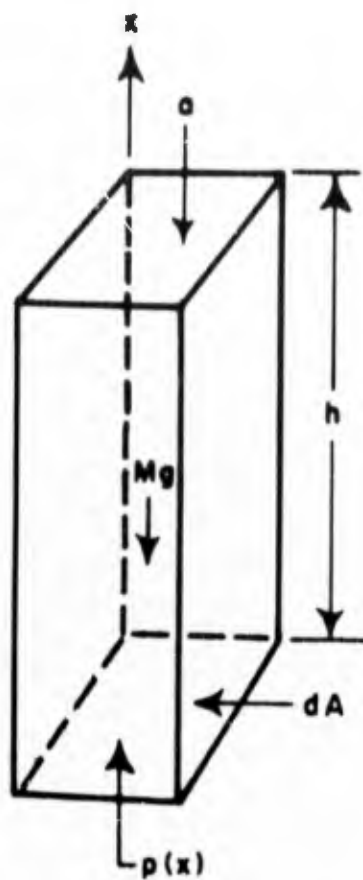


Figure 33. Elemental Volume of Overburden

$$p(x) = (p_o + a) \left(\frac{x}{x_o} \right)^{-\gamma} \quad (17)$$

a = atmospheric pressure

m = overburden mass/dA

$$\frac{d^2x}{dt^2} - \left(\frac{p_o + a}{M} \right) \left(\frac{x}{x_o} \right)^{-\gamma} + \frac{a}{M} + g = 0 \quad (18)$$

For the primacord technique, p_o was assumed to be the peak pressure obtained from a least-square fit of the observed pressure-time history. For the detonation technique, p_o is a function of time and is obtained from the expansion calculation described in section IV of the report.

Numerical integration had to be used to solve this nonlinear differential equation. A Kutta-Gill approximation to a Taylor series was used to start the computation. The equations used for this method are derived in reference 6. These equations are

$$\ddot{x} = \frac{d^2x}{dt^2} = G(t, x, \dot{x}) \quad (19)$$

$$x_{n+1} = x_n + h\dot{x}_n + \frac{h}{6} (m_o + m_1 + m_2) + O(h^5) \quad (20)$$

$$\dot{x}_{n+1} = \dot{x}_n + \frac{1}{6} (m_o + 2m_1 + 2m_2 + m_3) + O(h^5) \quad (21)$$

$$m_o = hG(t_n, x_n, \dot{x}_n) \quad (22)$$

$$m_1 = hG\left(t_n + \frac{1}{2}h, x_n + \frac{1}{2}h\dot{x}_n, \dot{x}_n + \frac{1}{2}m_o\right) \quad (23)$$

$$m_2 = hG\left(t_n + \frac{1}{2}h, x_n + \frac{1}{2}h\dot{x}_n + \frac{1}{4}m_o h, \dot{x}_n + \frac{1}{2}m_1\right) \quad (24)$$

$$m_3 = hG\left(t_n + h, x_n + h\dot{x}_n + \frac{1}{2}m_1 h, \dot{x}_n + m_2\right) \quad (25)$$

$$h = \text{time increment} = 0.0001 \text{ second} \quad (26)$$

These equations were used to obtain the first four points. Next, Milne's method, which uses Simpson's 1/3 Rule, was used to continue the computation. The computer program used to make these computations may be found at the end of this appendix. Table V defines the information that must be read into the program:

Table V

PROGRAM CONSTANTS

T(2)	Initial time = 0
X(2)	Initial displacement (inches) = x_0
$\dot{X}(2)$	Initial velocity = 0
H	Time increment = 0.0001 seconds
TLIM	Cutoff time
INCOUT	Time increment between print out
PS	Overburden mass, lbm/ft^3
X_0	Cavity depth, inches
G1	Ratio of specific heats = 1.3

These computations are greatly simplified by three assumptions. First, the ratio of specific heats is considered to be constant. Second, the expansion is assumed to be isentropic and to involve an ideal gas. Finally, no account is made for the motion of the earth being loaded. These effects can be substantial. The whole purpose of making these duration calculations has been to get a qualitative estimate of the effect of varying the cavity depth and the mass of the surcharge. Accurate duration predictions must come from experimental data.

COMPUTER PROGRAM

```

C      PROGRAM DISP
      DIMENSION T(5000),X(5000),XDOT(5000),ACC(5000),PL(5000)
5     READ 105,T(2),X(2),XDOT(2),PMAX,H,TLIM,PS,INCOUT
      PRINT 106,T(2),X(2),XDOT(2),H,TLIM,INCOUT
      CALL ALOAD (T(2),2,X(2),AL)
      P(2) = AL
      A = 14.7
      AM = PS/(386.*144.)
      G = 386.*A/AM
      K = 1
      ACC(2) + (PMAX/AM)-G
      PRINT 112,AM,ACC(2)
20    DO 50 N = 2,4
22    CALL ALOAD(T(N),3,X(N),AL)
      AMO = H*ACSELF(AL,AM,G)
24    CALL ALOAD(T(N)+0.5*H,3,X(N)+0.5*H*XDOT(N),AL)
      AM1 = H*ACSELF(AL,AM,G)
26    CALL ALOAD(T(N)+0.5*H,3,X(N)+0.5*H*XDOT(N)+0.25*H*AMO,AL)
      AM2 = H*ACSELF(AL,AM,G)
28    CALL ALOAD(T(N)+H,3,X(N)+H*XDOT(N)+0.5*H*AM1,AL)
      AM3 = H*ACSELF(AL,AM,G)
      NN = N+1
      T(NN) = T(N)+H
      X(NN) = X(N)+H*XDOT(N)+H*(AMO+AM1+AM2)/6.
      XDOT(NN) = XDOT(N)+(AMO+2.*(AM1+AM2)+AM3)/6.
      CALL ALOAD (T(NN),3,X(NN),AL)
      P(NN) = AL
      ACC(NN) = ACSELF(AL,AM,G)
50    CONTINUE
      DO 70 M = 6,5000
      M1 = M
      XDOT(M) = XDOT(M-4)+(4./3.)*H*(2.*ACC(M-1)-ACC(M-2)+2.*ACC(M-3))
      X(M) = X(M-2)+(H/3.)*(XDOT(M)+4.*XDOT(M-1)+XDOT(M-2))
      T(M) = T(M-1)+H

```

COMPUTER PROGRAM (cont'd)

```

51 CALL ALOAD(T(M),3,X(M),AL)
   PL(M) = AL
   ACC(M) = ACCEL F(AL,AM,G)
   XDOT(M) = XDOT(M-2)+(H/3.)*(ACC(M)+4.*ACC(M-1)+ACC(M-2))
   X(M) = X(M-2)+(H/3.)*(XDOT(M)+4.*XDOT(M-1)+XDOT(M-2))
   CALL ALOAD(T(M),3,X(M),AL)
   ACC(M) = ACCEL F(AL,AM,G)
   GO TO (52,56),K
52 IF(X(M)-X(M-1))54,54,70
54 PRINT 107,X(M-1),T(M-1)
   K = 2
56 IF(T(M)-TLIM)70,76,76
70 CONTINUE
76 MM = INCOUT+2
   PRINT 109
   PRINT 110,T(2),ACC(2),XDOT(2),X(2)
78 PRINT 111,T(MM),ACC(MM),XDOT(MM),X(MM),PL(MM)
   IF(MM+INCOUT-M1)80,83,83
80 MM = MM+INCOUT
   GO TO 78
83 IF(M1-5000)5,85,85
85 IF(T(5000)-TLIM)87,5,5
87 T(2) = T(5000)
   X(1) = X(4999)
   X(2) = X(5000)
   XDOT(2) = XDOT(5000)
   ACC(2) = ACC(5000)
   GO TO 20
105 FORMAT(7F10.5,I2)
106 FORMAT(1H1 // 1H2 20X 23H INITIAL CONDITIONS ARE // 25X 7H TIME =
1F18.3, 9H SECONDS / 25X 15H DISPLACEMENT = F10.3, 8H INCHES / 25X
2,11H VELOCITY = F14.3, 17H INCHES / SECOND // 25X 32H TIME INCREM
3ENT OF INTEGRATION = F9.5, 10H SECONDS //25X 14H CUTOFF TIME = F
46.2,10H SECONDS // 25X 6H EVERY 15, 33H COMPUTATION(S) ARE PRI
5NTED OUT////)
107 FORMAT (//// 20X 24H MAXIMUM DISPLACEMENT IS F10.5, 17H INCHES, A
1T TIME F10.5, / 25X 10H SECONDS.)

```

COMPUTER PROGRAM (cont'd)

```

109 FORMAT (1H1 // 1H2 34X 5H TIME 7X 13H ACCELERATION 7X 9H VELOCITY
16X 14H DISPLACEMENT 20X 2H P /// 33X 8H SECONDS 5X 14H IN /(SEC)
2SQD 8X 9H IN / SEC 5X 7H INCHES////)
110 FORMAT (28X,F13.5,F18.5,2F17.5)
111 FORMAT(26X F15.5,F18.5,2F17.5,5X,F17.5)
112 FORMAT(1H2,25X,8H MASS = ,F10.5/25X,24H INITIAL ACCELERATION = ,F1
12.5)
END
SUBROUTINE ALOAD(T,N1,X,ANS1)
A = 14.7
IF(N1-2)115,105,115
105 READ 1000,X0,G1,PR
115 PT = PR+A
ANS1 = PT*((X/X0)**(-G1))
150 RETURN
1000 FORMAT(3F10.5)
END
FUNCTION ACCELF(X,Y,Z)
ACCELF = (X/Y)-Z
RETURN
END
*LAST
*DATA
1EOF

```

This page intentionally left blank.

APPENDIX II

INSTRUMENTATION

1. General

The design of the instrumentation system for Phase I was based upon the parameters to be measured, the availability and location of equipment, the requirement for the use of long lines, and the field conditions under which the tests were conducted. The parameters to be measured included air pressure, soil pressure, soil acceleration, detonation-wave velocity and profile, overburden motion, and initial pit temperature. Because of the explosive nature of the tests, the test facility was located 500 feet from the available recording equipment. This required long lines for signal transmission.

The recording equipment used during this test series was located in the Air Force Shock Tube Facility. Field conditions required that gages and cables be used which were compatible with dust, moisture, and other adverse field environments. The use of any piezoelectric gages was rejected because of the long line problem and because of the possibility of encountering moisture. It was decided that wherever possible, resistance-bridge-type gages would be used.

A complete recapitulation of instrument characteristics is given in table V at the end of this appendix.

2. Air Pressure

The time history of the air pressure at the surface of the ground had to be measured. This would give time of arrival of the detonation wave, peak pressure, and pressure decay profile. The first gage selected for use in these tests was the Kulite-Bytrex HF 500 pressure cell. This is a small semiconductor resistance-bridge gage with extremely high natural frequency (100 kc). It consists of a small pressure cell and a bridge completion module connected by small wires. This gage was selected after shock tube tests showed that it had a sufficiently high-frequency response to prevent excessive ringing when subjected to a shock wave. However, the gage proved to be too delicate and unsuitable for use in the field. In addition, the very thin pressure diaphragm of this gage was easily driven off range by any material placed on the gage.

The second gage selected for use in the Phase I tests was the Norwood, both Models 111 and 211. This gage is a very rugged, conventional resistance-bridge device having a natural frequency of 45 kc. Although these gages rang somewhat in blast tests, they provided suitable air pressure data and were rugged enough to be used on repeated tests. The air pressure gages were mounted in metal housings which were imbedded in the surface of the ground. The gages were shock isolated from the metal housings with nylon mounting grommets. The metal housings were waterproofed.

3. Soil Pressure

The Lynch Soil Stress gage, recently developed at the Air Force Shock Tube Facility, was used to measure the pressure-time history in the soil. This gage contains a semiconductor strain gage bridge mounted on a small right circular cylinder. The cylinder is located in the gage housing such that soil pressure acts to compress the cylinder and the strain gage. These gages were placed at various depths below the surface of the ground from 3 inches to 25 feet. The gages were placed at the selected depth in an 8-inch-diameter drill hole and then sand was rained into the hole.

4. Soil Acceleration

Accelerometers were placed inside waterproof, aluminum canisters and installed at various depths in 8-inch drilled holes. Back filling was again accomplished with rained sand. The Pace model A-18 accelerometer was selected for these tests because it had been used successfully at the Nevada Test Site. It is a variable-reluctance-type accelerometer with a high signal output. Its frequency response is only average but sufficient for this test series. It was driven with a 3-kc carrier system. A few Statham model A-5 accelerometers were also used. The accelerometers were oriented to measure vertical accelerations at various depths in 3 25-foot-deep drill holes.

5. Surcharge Motion

High-speed movie cameras were used on each test to record the motion of the overburden. Target stands were placed both on top and at the base of the overburden material so the relative motion of the top and the bottom of the surcharge material could be observed.

On some tests, a high-speed camera was located on a boom above the pit to photograph the detonation wave.

6. Recording

Signal conditioning for the variable reluctance gages was provided by a CEC System "D" 3-kc carrier system. Signal conditioning for the other gages was provided by Allegany Instruments Sensor Analog Modules (SAM-1) and Astro Data Model TDAB74 amplifiers with battery gage excitation. The SAM-1 unit is a gage power supply, dc wideband amplifier, bridge balance and calibration device combined in one module.

The output from the signal conditioning systems was fed through a patch panel to Ampex CP-100 FM tape recorders. Timing control and serial time code was supplied by the instrumentation recording complex at the Air Force Shock Tube Facility.

Belden six-wire shielded instrumentation cable was used for the long lines connecting gages to signal conditioning equipment.

7. Problems

Some setbacks were encountered in the instrumentation of the Phase I tests. Continued difficulty was encountered with air pressure gage mounting. On several tests it appeared as though the gage housings had been pulled from the ground by rebounding of the earth's surface after compression. There was almost always cable damage to the air pressure gages. Later housing designs reduced this problem.

On one test, the movement of the soil inside the test pit downward along the concrete wall sheared the cables at the point where they passed through the wall. On later tests the cables were placed in plastic pipe and buried at a depth of 3 feet to protect them from this shearing action.

Waterproofing of cable splices remained a problem throughout the test series. Water entering a splice joint is carried down the cable and into the gage housing by capillary action. Summer rainstorms provided sufficient water to create a substantial problem.

Table VI

PHASE I, INSTRUMENTATION EQUIPMENT LIST

I. Tape Recorder

A. Make: Ampex

Model: CP-100

Ampex Corporation Instrumentation Products
934 Charter Street, Redwood City, California

List of Characteristics:

1. Tape Transport

- a. Tape Speeds: 60, 30, 15, 7-1/2, 3-3/4, 1-7/8 ips standard
- b. Tape Speed Deviation: ± 0.35 percent maximum
- c. Start Time: 5 seconds or less at 60 ips or 30 ips
3 seconds or less at 15 ips or 7-1/2 ips
1.5 seconds or less at 3-3/4 ips or 1-7/8 ips
- d. Stop Time: Maximum of 2.0 seconds

2. Direct Record/Reproduce System

a. Frequency Response and RMS Signal-to-Noise Ratio:

<u>Tape Speed</u> <u>(ips)</u>	<u>Bandwidth</u> <u>(cps)</u>	<u>RMS Signal to RMS Noise</u>	
		<u>Bypass</u> <u>(db) Filtered</u>	<u>Unfiltered</u> <u>Wideband (db)</u>
60	300 to 250,000 ± 3 db	30	25
30	200 to 125,000 ± 3 db	30	24
15	200 to 60,000 ± 3 db	30	23
7-1/2	200 to 25,000 ± 3 db	28	21
3-3/4	200 to 12,000 ± 3 db	28	19
1-7/8	200 to 6,250 ± 3 db	28	19

b. Input Level: 1.0 volt rms nominal to produce recording level; operable from 0.7 to 10.0 volts rms.

c. Input Impedance: Minimum 18,000 ohms resistive, in parallel with 275 micromicrofarads, unbalanced to ground.

d. Output Level: 1.0 volt rms nominal across a 10,000 ohms or greater impedance.

e. Output Impedance: Less than 100 ohms.

f. Control Track Generator: Subcarrier frequency 17 kc or 18.24 kc. Modulating frequency 60 cps ± 0.02 percent. Modulation 50 \pm 5 percent.

3. Power Requirements

a. Voltage: 105 to 125 volts, single phase, 48 to 62 cps or 380 to 420 cps a.c.; or 210 to 250 volts, single phase, 48 to 62 cps or 380 to 420 cps a.c.; or 26 to 30 volts d.c., ripple 2 volts peak-to-peak maximum.

b. Power Consumption: Approximately 375 watts for a 14-track system.

4. Environment

a. Temperature: Operating $+40^{\circ}\text{F}$ to $+125^{\circ}\text{F}$. Storage/Nonoperating -20°F to 160°F .

b. Altitude: Operating 10,000 feet; nonoperating 20,000 feet.

c. Relative Humidity: Up to 95 percent without condensation space.

II. Amplifier

A. Make: Astrodata

Model: TDA 874

Astrodata, Inc.

240 E. Palais Road, Anaheim, California

List of Characteristics:

1. Gain Range: 1 to 5,000 in steps of 1,000, 500, 200, 100, and 50. Frequency response is inversely proportional to gain, e.g., at a gain of 3,000 the frequency response is down to 3 db at 75 kc.

2. Gain Accuracy: ± 0.02 percent, d.c. to 1 kc into open circuit at 25°C .

3. Gain Stability: ± 0.01 percent, d.c. to 100 cps for six months at 25°C .

4. Linearity: ± 0.01 percent, d.c. to 1 kc.

5. Input Impedance: Greater than 100 megohms shunted by 0.0007 microfarad.

6. Output Voltage: ± 10 volts, limited at less than ± 13 volts, d.c. to 10 kc.

7. Output Current: ± 100 milliamperes, d.c. to 10 kc.
8. Output Impedance: Less than 1 ohm in series with 50 microhenties.
9. Rated Load Resistance: 200 ohms.
10. Capacitive Load: 0.02 microfarad.
11. Frequency Response: ± 0.1 db, d.c. to 10 kc, down 3 db at 150 kc.
12. Drift: 40 hours, ± 2 microvolts referred to the input. Six months, ± 4 microvolts referred to the input.
13. Noise: Less than 5 microvolts rms referred to the input plus 150 microvolts rms referred to the output from 0.05 cps to 30 kc at 25°C.
14. Common Mode Rejection: Greater than 140 db at d.c., 120 db at 60 cps, 100 db at 400 cps for 1,000 ohms or less of source resistance unbalance.

III. Signal Conditioning Equipment

A. Make: Consolidated Electrodynamics Corporation

Model: CEC System D (Type 1-113B Carrier Amplifier)

Consolidated Electrodynamics Corporation, Data Recorders Division
360 Sierra Madre Villa, Pasadena, California

List of Characteristics:

1. Full-Scale Output: ± 5 ma into a 26-ohm load.
2. Sensitivity: Input signal for maximum output, 1 mv with no attenuation, 1 volt maximum with full attenuation.
3. Input Impedance: Approximately 1,800 ohms.
4. Input Attenuator: 1 to 1,000 in 20 steps.
5. Bridge Balance System: Will accommodate four external bridge arms composed of wire strain gages or other resistance elements or two-arm variable-reluctance transducers suitable for use at 3 kc.
6. Linearity: Output current proportional to input voltage within 2 percent of maximum output.
7. Frequency Response: Galvanometer trace amplitude constant (± 2 percent) for modulating frequencies from 0 to 600 cps.

B. Make: Allegany

Model: SAM-1

Allegany Instrument Company, Division of Textron Electronics, Inc.
1091 Wills Mountain, Cumberland, Maryland

List of Characteristics:

1. Gain Range: 100 to 2,000, continuous with vernier.
2. Amplifier Balance Control Range: ± 1.00 microvolts referred to the input.
3. Balance Range: ± 10 percent of scale standard.
4. Linearity: 0.02 percent of full scale at d.c.
5. Frequency Response: d.c. to 40 kc. Down 3 db at 40 kc with vernier fully counterclockwise.
6. Noise: 7 microvolts rms, d.c. to 40 kc. Two microvolts peak-to-peak, d.c. to 3 cps.
7. Drift: 0.3 microvolt/ $^{\circ}$ F referred to input.
8. Output Impedance: Less than 0.1 ohm at d.c.
9. Output Voltage: 10 volts d.c. or peak a.c. to 20 kc.
10. Output Current: 100 ma d.c.
11. Common Mode Rejection: 90 db at 60 cps.

IV. Air Pressure Gage

A. Make: Norwood

Model: 111 Bonded Strain Gage Pressure Transducer

Advanced Technology Laboratories, a Division of American-Standard
369 Whisman Road, Mountain View, California

List of Characteristics:

1. Nonlinearity: Better than 0.5 percent of F.S. by terminal method or 0.25 percent by best straight line through zero method.
2. Hysteresis: Better than 0.5 percent of F.S.
3. Repeatability: Better than 0.1 percent of F.S.

4. Resolution: Infinite.
5. Acceleration Effect: Less than 0.1 percent F.S. per g in all planes.
6. Vibration Effect: Insensitive from 50 to 2,000 cps to 100 g in 3 planes.
7. Zero Pressure Output: Less than ± 2 percent of F.S. at rated excitation.
8. Resonant Frequency: Approximately 45,000 cps.
9. Frequency Response: Flat within \pm db from 0 to 20,000 cps.
10. Pressure Limit: 150 percent of F.S. for static pressures (125 percent for 100 psi range). Full scale for dynamic pressures.
11. Recommended Excitation: 10 volts d.c. or a.c., 17 volts maximum.
12. Electrical Output: 3.5 mv/v ± 20 percent for -34 bridge, 3.0 mv/v ± 2 percent for -35 and -36 bridge.

B. Make: Norwood

Model: 211 General Purpose Bonded Strain Cage Pressure Transducers
Advanced Technology Laboratories, a Division of American-Standard
369 Whisman Road, Mountain View, California

List of Characteristics:

1. Nonlinearity and Hysteresis: Less than 0.75 percent of F.S. by best straight line through curve method, 5,000 to 10,000 psi units less than 1 percent.
2. Repeatability: Within 0.1 percent of F.S.
3. Resolution: Infinite.
4. Zero Pressure Output: Less than ± 15 percent of F.S.
5. Resonant Frequency: Approximately 45,000 cps.
6. Pressure Limit: 150 percent of F.S. for static pressures, full scale for dynamic pressures.
7. Recommended Excitation: 10 volts d.c. or a.c., 17 volts maximum.

C. Make: Kulite-Bytrex

Model: HF-500

Bytrex Corporation, Kulite-Bytrex Corporation
50 Hunt Street, Newton, Massachusetts

List of Characteristics:

1. Output Signal: 100 mv F.S. minimum.
2. Output Impedance: 1,300 ohms at 80°F, increase approximately 0.015 percent/°F.
3. Input Impedance: 500 ohms at 80°F, increase approximately 0.06 percent/°F.
4. Excitation: 20 volts d.c. or a.c. rms.
5. Natural Frequency: 80 kc.
6. Shock: Will withstand more than 2,500 g on all axes.
7. Acceleration Sensitivity: 0.002 percent per g.
8. Operating Temperature Range: -65 to +300°F.
9. Nonlinearity and Hysteresis: Less than 1 percent, combined.
10. Maximum Allowable Pressure: 150 percent of range without damage, 200 percent of range without rupture.
11. Measuring Range: 0 to 500 psig.

V. Accelerometers

A. Make: Statham

Model: A5-200-350

Statham Instruments, Inc.
12401 W. Olympic Blvd, Los Angeles, California

List of Characteristics:

1. Acceleration Range: ± 200 g.
2. Bridge Resistance: 350 ohms.
3. Excitation: 11 volts d.c. or a.c. rms.
4. Full Scale Output: Approximately ± 44 mv.
5. Operating Temperature Range: -40°F to +20 °F.
6. Direction of Sensitivity: Perpendicular to base.

7. Overload: Three times rated range.

8. Transverse Acceleration Response: Less than 0.02g/g for transverse accelerations up to rated range.

9. Nonlinearity and Hysteresis: Less than +1 percent of F.S. output.

10. Natural Frequency: Approximately 850 cps.

VI. Soil Pressure Gages

A. Make: Lynch

Model: Developed and fabricated in Air Force Shock Tube Facility

List of Characteristics:

1. Frequency Response: Greater than 100 kc.

2. Range: 0 to greater than 2,000 psi.

VII. Cable

A. Make: Belden

Model: 8777 (Belden 6-wire)

Belden Manufacturing Company
P. O. Box 5070A, Chicago, Illinois

List of Characteristics:

1. Gage of Wire: 22.

2. Suggested Working Voltage: 300 volts.

3. Capacitance between Conductors: 300 mmf/ft.

4. Capacitance between Adjacent Shields: 115 mmf/ft.

5. Resistance between Shields: 100 megohms/M.

6. Voltage Breakdown between Adjacent Shields: 1,500 volts.

7. Working Voltage between Adjacent Shields: 50 volts.

REFERENCES

1. Crosby, J. K., et al., Feasibility of Simulating the Mechanical Effects of a Nuclear Explosion Using Non-Nuclear Explosives, DASA-1264, December 31, 1961.
2. D'Arcy, Gerald P., Clark, Robert O., Simulation of Air Shocks with Detonation Waves, AFWL TR-65-9, AF Weapons Laboratory, Kirtland AFB, New Mexico (to be published).
3. Taylor, J., Detonation in Condensed Explosives, Oxford University Press, London, 1952.
4. Courant, R., Friedrichs, K. D., Supersonic Flow and Shock Waves, Interscience Publishers, Inc., New York, 1948.
5. Kruz, F. R., Draft of Final Report "Investigation of Air Blast Induced Ground Motion Technique Using High Explosives," unpublished report by the MRD Divison, GATC, to the AFWL, Kirtland AFB, New Mexico, 1964.
6. Kent, R. B., "The Single Degree of Freedom System as a Mathematical Model for Dynamically Loaded Footings on Sand," Ph.D. dissertation, University of Florida (to be published).

DISTRIBUTION

No. cys

HEADQUARTERS USAF

Hq USAF, Wash, DC 20330

- 2 (AFOCE)
- 1 (AFTAC)
- 1 (AFRDPF, Maj Dunn)

MAJOR AIR COMMANDS

AFSC, Andrews AFB, Wash, DC 20331

- 1 (SCT)
- 1 (SCLT)
- 1 (SCMC)
- 1 SAC (DORQM), Offutt AFB, Nebr 68113
- 1 AUL, Maxwell AFB, Ala 36112
- 2 USAFIT, Wright-Patterson AFB, Ohio 45433
- 2 USAFA, Colo 80840

AFSC ORGANIZATIONS

- 1 FTD (TDBTL), Wright-Patterson AFB, Ohio 45433
- RTD, Bolling AFB, Wash, DC 20332
- 1 (RTN)
- 1 (RTN-W, Lt Col Munyon)
- 1 (RTS)
- 1 AEDC (AEYD), Arnold AFS, Tenn 37289
- BSD, Norton AFB, Calif 92409
- 2 (BSQ)
- 1 (BSR)
- 1 (BSOT)
- 2 (BSSF)
- 1 ESD (ESTI), L. G. Hanscom Fld, Bedford, Mass 01731

KIRTLAND AFB ORGANIZATIONS

AFSWC, Kirtland AFB, NM 87117

- 1 (SWEH)
- 1 (SWT)

DISTRIBUTION (cont'd)

No. cys

AFWL, Kirtland AFB, NM 87117

15 (WLIL)

1 (WLA)

1 (WLD)

20 (WLDC)

1 (WLR)

1 SAC Res Rep (SACLO), AFSWC, Kirtland AFB, NM 87117

OTHER AIR FORCE AGENCIES

Director, USAF Project RAND, via: Air Force Liaison Office, The RAND Corporation, 1700 Main Street, Santa Monica, Calif 90406

1 (RAND Physics Div, Dr. Hal Brode)

1 (RAND Library)

1 SACSO, Norton AFB, Calif 92409

ARMY ACTIVITIES

1 Director, Ballistic Research Laboratories (Library), Aberdeen Proving Ground, Md 21005

1 Commanding Officer (SMVPA-VA6), Picatinny Arsenal, Samuel Feltman Ammunition Laboratories, Dover, NJ 07801

1 Commandant, Command and General Staff College (Archives), Ft Leavenworth, Kans 66027

1 Chief of Engineers (ENGMC-EM), Department of the Army, Wash, DC 20315

1 Director, Army Research Office, 3045 Columbia Pike, Arlington, Va 22204

1 Director, US Army Waterways Experiment Sta (WESRL), P. O. Box 631, Vicksburg, Miss 39181

NAVY ACTIVITIES

1 Chief of Naval Research, Department of the Navy, Wash, DC 20390

1 Chief, Bureau of Naval Weapons (RRNU), Department of the Navy, Wash, DC 20360

1 Bureau of Yards and Docks, Department of the Navy, Code 22.102 (Branch Manager, Code 42.330), Wash 25, DC

1 Bureau of Ships, Department of the Navy (Melvin L. Ball, Code 1500), Wash, DC 20360

1 Commanding Officer, Naval Research Laboratory, Wash, DC 20390

1 Superintendent, US Naval Postgraduate School, ATTN: George R. Luckett, Monterey, Calif

DISTRIBUTION (cont'd)

No. cys

- 1 Commanding Officer and Director, Naval Civil Engineering Laboratory, Port Hueneme, Calif
- 1 President, US Naval War College, Newport, RI
- 1 Office of Naval Research, Wash, DC 20360

OTHER DOD ACTIVITIES

- 2 Director, Defense Atomic Support Agency (Document Library Branch), Wash, DC 20301
- 1 Commander, Field Command, Defense Atomic Support Agency (FCAG3, Special Weapons Publication Distribution), Sandia Base, NM 87115
- 1 Director, Advanced Research Projects Agency, Department of Defense, The Pentagon, Wash, DC 20301
- 1 Office of Director of Defense Research and Engineering, ATTN: John E. Jackson, Office of Atomic Programs, Rm 3E1071, The Pentagon, Wash, DC 20330
- 1 Chairman, Armed Services Explosives Safety Board, Wash 25, DC
- 1 US Documents Officer, Office of the US National Military Representative (SHAPE), APO 55, New York, NY
- 50 DDC (TIAAS), Cameron Station, Alexandria, Va 22314

AEC ACTIVITIES

- 1 US Atomic Energy Commission (Headquarters Library, Reports Section), Mail Station G-017, Wash, DC 20545
- 1 Sandia Corporation (Technical Library), P. O. Box 969, Livermore, Calif 94551
- 1 University of California Lawrence Radiation Laboratory (Technical Information Division, ATTN: Dr. R. K. Wakerling), Berkeley 4, Calif
- 1 Director, Los Alamos Scientific Laboratory (Helen Redman, Report Library), P. O. Box 1663, Los Alamos, NM 87554

OTHER

- 2 OTS (CFSTI, Chief, Input Section), Sills Bldg, 5285 Port Royal Road, Springfield, Va 22151
- 1 Office of Assistant Secretary of Defense (Civil Defense), Wash, DC 20301
- 1 Institute for Defense Analysis, Rm 2B257, The Pentagon, Wash, DC 20330

THRU: ARPA

- 1 Aerospace Corporation, P. O. Box 95085, Los Angeles 45, Calif
- 1 Aerospace Corporation, ATTN: Mr. Ivan Weeks, Ballistic Missile Division, San Bernardino, Calif

DISTRIBUTION (cont'd)

No. cys

- 2 AF Shock Tube Facility, ATTN: Dr. Zwoyer, Box 188, University Station, Albuquerque, NM
- 1 University of Illinois, Civil Engineering Dept, ATTN: Dr. N. M. Newmark, Head, Talbot Laboratory, Urbana, Ill
- 1 Space Technology Laboratoryies, Inc., AF Contr Mgt Office, c/o STLTD, Bldg S/1930, One Space Park, Redondo Beach, Calif 90278
- 1 Official Record Copy (Capt Gerald P. D'Arcy, WLDC)

This page intentionally left blank.

UNCLASSIFIED
Security Classification

DOCUMENT CONTROL DATA - R&D		
(Security classification of title, body of abstract and indexing annotation must be entered when the overall report is classified)		
1 ORIGINATING ACTIVITY (Corporate author) Air Force Weapons Laboratory (WLDC) Kirtland Air Force Base, New Mexico 87117		2a REPORT SECURITY CLASSIFICATION UNCLASSIFIED 2b GROUP
3 REPORT TITLE SIMULATION OF AIR-BLAST-INDUCED GROUND MOTION		
4 DESCRIPTIVE NOTES (Type of report and inclusive dates) December 1963-August 1964		
5 AUTHOR(S) (Last name, first name, initial) D'Arcy, Gerald P.; Auld, Harry E.; Leigh, Gerald G. Captain, USAF Captain, USAF Captain, USAF		
6. REPORT DATE April 1965	7a. TOTAL NO. OF PAGES 84	7b. NO. OF REFS 6
8a. CONTRACT OR GRANT NO. b. PROJECT NO. 5710 c. WEB No. 13.166 d.	9a. ORIGINATOR'S REPORT NUMBER(S) AFWL TR-65-11 9b. OTHER REPORT NO(S) (Any other numbers that may be assigned this report)	
10 AVAILABILITY/LIMITATION NOTICES DDC release to OTS is authorized.		
11. SUPPLEMENTARY NOTES	12. SPONSORING MILITARY ACTIVITY AFWL (WLDC) Kirtland AFB, NM 87117	
13. ABSTRACT An analytical and experimental program was performed to determine the most promising techniques for simulating the air-blast-induced ground motions from a large-yield nuclear weapon. Two techniques were then selected for further development. One of the selected techniques employs a detonable gas mixture and the other a primacord matrix to generate a traveling shock wave which loads the ground. The nuclear air-blast overpressure environment is described and the simulation produced by either scheme is compared with this environment. The primacord technique was then selected because it was found to be the most practical and economical. Sufficient data are presented to enable the design of simulation experiments which use either technique.		